Nonlinear Dyn (2024) 112:21321–21341
https://doi.org/10.1007/s11071-024-10036-9

RESEARCH

Qualitative analysis and optical soliton solutions galore: scrutinizing the (2+1)-dimensional complex modified Korteweg–de Vries system

Bahadır Kopçasız

Received: 5 May 2024 / Accepted: 15 July 2024 / Published online: 30 August 2024
© The Author(s) 2024

Abstract This investigation discusses the (2+1)-dimensional complex modified Korteweg–de Vries (cmKdV) system. The cmKdV system describes the nontrivial dynamics of water particles from the surface to the bottom of a water layer, providing a more comprehensive understanding of wave behavior. The cmKdV system finds applications in various fields of physics and engineering, including fluid dynamics, nonlinear optics, plasma physics, and condensed matter physics. Understanding the behavior predicted by the cmKdV system can lead to insights into the underlying physical processes in these systems and potentially inform the design of novel technologies. A new version of the generalized exponential rational function method (nGERFM) is utilized to discover diverse soliton solutions. This method uncovers analytical solutions, including exponential function, singular periodic wave, combo trigonometric, shock wave, singular soliton, and hyperbolic solutions in mixed form. Moreover, the planar dynamical system of the concerned equation is created, all probable phase portraits are given, and sensitive inspection is applied to check the sensitivity of the considered equation. Furthermore, after adding a perturbed term, chaotic and quasi-periodic behaviors have been observed for different values of parameters, and multistability is reported at the end. To gain a deeper understanding of the dynamic behavior of the solutions, analytical results are supplemented with numerical simulations. These obtained outcomes provide a foundation for further investigation, making the solutions useful, manageable, and trustworthy for the future development of intricate nonlinear issues. This study's methodology is reliable, strong, effective, and applicable to various nonlinear partial differential equations (NLPDEs). As far as we know, this type of research has never been conducted to such an extent for this equation before. The Maple software application is used to verify the correctness of all obtained solutions.

B. Kopçasız (✉)
Department of Mathematics, Faculty of Arts and Sciences, Bursa Uludag University, 16059 Bursa, Turkey
e-mail: bkopcasz@gmail.com

1 Introduction

In the modern era, NLPDEs and their solutions have become more interesting and challenging research areas for mathematicians and research communities. These play a significant role in the study of nonlinear physical phenomena in mathematical studies and applied physics, with essential applications in several areas of engineering and natural science. Exact or analytical solutions have been the focus of scholars due to their essential contribution to the analysis of the real features of nonlinear problems. Due to its wide utilization and applications in the domain of nonlinear sciences, a momentous consideration for studying NLPDEs has been increased [1–3]. Therefore, extracting solitary wave solutions to NLPDEs is becoming a fascinating field in the nonlinear sciences day by day. Numerous NLPDEs can be solved using

various mathematical strategies such as extended simplest equation method [4], improved auxiliary equation technique [5], modulation instability [6], F-expansion technique [7], modified Sardar sub-equation method [8], unified method [9], extended rational sine-cosine/sinh-cosh method [10], generalized exponential rational function method (GERFM) [11], extended sinh-Gordon equation expansion method [12], generalized Kudryashov method [13], $\left(\frac{G'}{G^2}\right)$-expansion method [14], modified Khater method [15], advanced auxiliary equation method [16], (w/g)-expansion approach [17], extended hyperbolic function technique [18], modified extended auxiliary equation mapping (MEAEM) technique [19], polynomial expansion technique [20].

The KdV equation is a partial differential equation (PDE) that mathematically represents waves in shallow water. It is notable for being the classic illustration of an integrable PDE, exhibiting many of the common characteristics, including an abundance of explicit solutions, especially soliton solutions, and an infinite number of conserved quantities. The equation has a wide range of applications, including the evolution of long, one-dimensional waves in many physical contexts. Its original intent was to describe shallow water waves with weakly non-linear restoring forces. The KdV equation is a significant mathematical model that possesses soliton solutions. Solitons are localized waves that can maintain their shape and speed even after colliding with other solitons. These waves have been extensively studied in the field of mathematical physics [21–23].

To determine the explicit and individual wave solutions of NLPDEs, the utilization of the traveling wave solution method is imperative. Soliton solutions are present in NLPDEs, representing a singular traveling wave [24–26]. Specifically, the equilibrium between the dispersion and nonlinear elements of nonlinear equations results in soliton solutions, sparking interest in solitary wave theory across various disciplines. Solitons maintain stability, remaining localized without dispersion and defying the principle of superposition. The concept of solitary waves in nonlinear mediums has garnered significant attention due to their utility in high-speed communications. Scholars have extensively examined the well-posedness of nonlinear models, with a focus on solitary and shallow water waves. Solitons propagate through monomode optical fibers, commonly used in long-distance communication networks and fiber optic-based ultra-fast pulse analysis devices. The prospect of transmitting high-bandwidth data over vast distances through large erbium-doped fiber amplifiers using optical solitons appears to be technically viable in the foreseeable future.

In mathematical physics, the cmKdV equation is important, especially when studying waves and solitons. By describing the nontrivial motions of water particles from a water layer's surface to its bottom, this equation helps to clarify wave behavior. A more thorough explanation of wave phenomena is possible thanks to the complex-valued extension of the classical KdV equation, known as the cmKdV system [27]. The cmKdV system is given by [28]:

$$\begin{aligned} &\psi_t + \psi_{xxy} + i\psi\varphi + (\psi\tau)_x = 0,\\ &\varphi_x + 2i\rho(\psi^*\psi_{xy} - \psi^*_{xy}\psi) = 0,\\ &\tau_x - 2\rho\left(|\psi|^2\right)_y = 0. \end{aligned} \tag{1}$$

Here, ψ, ψ^*, φ, and τ functions depends on x, y, t. Furthermore, ψ is a complex function, and its conjugate is ψ^*, φ and τ are real functions, $\rho = \pm 1$ and the partial derivatives for x, y, and t are symbolized by the subscripts. This prototype is a generalization of the cmKdV system in the $(2+1)$-dimension and has considerable significance for applied ferromagnetism and nanomagnetism [28].

Numerous investigations have used the Darboux transformation (DT) to examine the system (1). One-soliton and two-soliton solutions are acquired using DT, starting with the zero seed, according to Yesmakhanova et al. [29]. In Yuan et al. [30], deformed solitons are generated by n-fold DT. The method can be started using a plane wave seed to produce periodic line wave solutions and breather solutions [31]. Order-n-breather solutions are presented by Shaikhova et al. [32]. Still, none of the aforementioned investigations are traveling wave solutions. However, three approaches- the sine-cosine, Kudryashov, and tanh-coth methods- have been used in recent studies to build traveling wave solutions for the system (1) [33].

The main objective of this work is to construct novel optical soliton solutions for the system (1). We use the nGERFM, a new method that is the primary subject of our study, for this aim. One might easily conclude that the new approach is quite effective and successful in seeking the exact solutions of the NLPDEs. Moving beyond analytical solutions, we unveil intricate system behaviors through a comprehensive bifurcation analy-

sis using planar dynamical systems. Subsequently, the exploration delves into chaotic phenomena by introducing an external term to the system, followed by an investigation of two- and three-dimensional phase portraits to uncover complex dynamics. To ensure solution stability, sensitivity analysis using the Runge–Kutta method is performed against minor initial perturbations. Comprehensive bifurcation analysis and phase portraits of the unperturbed system are presented. The chaos analysis of the perturbed system employs various techniques to detect chaotic patterns in time series and phase portraits. The novelty of our investigation lies in its unprecedented nature within the discussed system's context. It leads readers on an exciting journey into the world of nonlinear waves and dynamical systems, offering additional revelations and insights.

The following are the remaining sections of this study: The Lax pair for the (2+1) dimensional cmKdV system is shown in Sect. 2. Section 3 presents the methodology of the selected method. Applications of the selected method are displayed in Sect. 4. Section 5 addresses qualitative analysis, which includes bifurcation analysis, sensitivity analysis, quasi-periodic and chaotic behaviors, and multistability analysis. Section 6 offers comparisons. Section 7 presents graphical explanations and Sect. 8 explains the conclusions.

2 The Lax pair system of the equation

For the system (1), the Lax pair system is

$$\Omega_x = K\Omega, \quad \Omega_t = 4\mu^2\Omega_y + M\Omega, \tag{2}$$

in which

$$K = \mu H + K_0, \quad M = \mu M_1 + M_0, \tag{3}$$

with

$$H = \begin{pmatrix} -i & 0 \\ 0 & i \end{pmatrix}, \quad K_0 = \begin{pmatrix} 0 & \psi \\ -s & 0 \end{pmatrix},$$

$$M_1 = \begin{pmatrix} i\tau & 2i\psi_y \\ 2is_y & -i\tau \end{pmatrix},$$

$$M_0 = \begin{pmatrix} -\frac{i\varphi}{2} & -\psi_{xy} - \tau\psi \\ s_{xy} + \tau s & \frac{i\varphi}{2} \end{pmatrix},$$

$$\Omega = \begin{pmatrix} \phi_1(\mu, x, y, t) \\ \phi_2(\mu, x, y, t) \end{pmatrix}.$$

The compatibility condition

$$K_t - M_x + KM - MK - 4\mu^2 K_y = 0 \tag{4}$$

infers the following cmKdV system:

$$\begin{aligned} &\psi_t + \psi_{xxy} + i\psi\varphi + (\tau\psi)_x = 0, \\ &s_t + s_{xxy} - i\varphi s + (\tau s)_x = 0, \\ &\varphi_x + 2i(s\psi_{xy} - s_{xy}\psi) = 0, \\ &\tau_x - (\psi s)_y = 0, \end{aligned} \tag{5}$$

in which φ, τ are real functions, ψ and s are complex functions. By setting $s = \rho\psi^*$ Eq. (5) become the cmKdV system (1).

3 Methodology

In this section, the procedures employed will be described. Consider the NLPDE as follows:

$$\begin{aligned} &Y_1[\psi(x, y, t), \frac{\partial}{\partial t}\psi(x, y, t), \frac{\partial}{\partial x}\psi(x, y, t), \\ &\quad \frac{\partial^2}{\partial t^2}\psi(x, y, t), \frac{\partial^2}{\partial x^2}\psi(x, y, t), \ldots] = 0. \end{aligned} \tag{6}$$

Using $\psi = \psi(x, y, t) = \Phi(\xi)$, and $\xi = x + y + ct$, Eq. (6) is transferred to

$$Y_2[c\Phi, \Phi'', \Phi''', \ldots] = 0. \tag{7}$$

3.1 Details of the nGERFM

This subsection provides the nGERFM-the revised methodology results in novel and differentiated findings [34].

Step 1 Let we set up the solution of Eq. (7) as:

$$\Phi(\xi) = k_0 + \sum_{n=1}^{n_0} k_n \left(\frac{\Lambda'(\xi)}{\Lambda(\xi)}\right)^n + \sum_{n=1}^{n_0} l_n \left(\frac{\Lambda'(\xi)}{\Lambda(\xi)}\right)^{-n}, \tag{8}$$

in which

$$\Lambda(\xi) = \frac{\varsigma_1 \exp(\jmath_1\xi) + \varsigma_2 \exp(\jmath_2\xi)}{\varsigma_3 \exp(\jmath_3\xi) + \varsigma_4 \exp(\jmath_4\xi)}. \tag{9}$$

In the pre-assumed structures Eqs. (9) and (8), $k_0, k_n, l_n (1 \le n \le n_0)$, and $\varsigma_i, \jmath_i$ $(1 \le i \le 4)$ are unknown coefficients. Further, to determine the positive integer n_0, we can use some known balancing rules in the literature.

Step 2 Inserting solution Eq. (8) into account in Eq. (7) introduces a polynomial equation $\Pi(\Xi_1, \Xi_2, \Xi_3, \Xi_4) = 0$ in terms of $\Xi_n = \exp(\jmath_v\xi)$ for $v = 1, 2, 3, 4$.

Step 3 Eventually, analytical solutions for Eq. (6) are obtained after insetting the results obtained from solving this system in the general structure Eq. (8).

4 Extraction of solution

The primary purpose of this section is to compile a diverse set of solutions to the given prototype. By operating wave transformation

$$\psi(x,y,t)=\Phi(x,y,t)\times\exp(i(b_1x+b_2y+b_3t)), \tag{10}$$

the system (1) reduces to ordinary differential equation (ODE):

$$\begin{aligned}&\Phi_t-2b_1b_2\Phi_x-b_1^2\Phi_y+\Phi_{xxy}+\Phi_x\tau+\Phi\tau_x\\&\quad+i\left(\left(b_3-b_1^2b_2\right)\Phi+2b_1\Phi_{xy}+b_2\Phi_{xx}\right.\\&\quad\left.+b_1\Phi\tau+\Phi\varphi\right)=0,\end{aligned} \tag{11}$$

$$\varphi_x-4\rho(b_2\Phi\Phi_x+b_1\Phi\Phi_y)=0, \tag{12}$$

$$\tau_x-2\rho(\Phi^2)_y=0. \tag{13}$$

Here b_1, b_2, and b_3 denote real constants.

Inserting the wave transformation

$$\psi(x,y,t)=\Phi(\xi)=\Phi(x+y+ct), \tag{14}$$

$$\varphi(x,y,t)=\varphi(\xi)=\varphi(x+y+ct), \tag{15}$$

$$\tau(x,y,t)=\tau(\xi)=\tau(x+y+ct), \tag{16}$$

in the system of (11)-(13), we get

$$\begin{aligned}&(c-2b_1b_2-b_1^2)\Phi'+\Phi'''+\Phi'\tau+\Phi\tau'\\&\quad+i\left(\left(b_3-b_1^2b_2\right)\Phi+(2b_1+b_2)\Phi''\right.\\&\quad\left.+b_1\Phi\tau+\Phi\varphi\right)=0,\end{aligned} \tag{17}$$

$$\varphi'-4\rho(b_2+b_1)\Phi\Phi'=0, \tag{18}$$

$$\tau'-2\rho(\Phi^2)'=0. \tag{19}$$

Integrating Eqs. (18) and (19) one time concerning ξ and taking integration to zero, we reach

$$\varphi=2\rho(b_2+b_1)\Phi^2,\qquad \tau=2\rho\Phi^2. \tag{20}$$

Substituting Eq. (20) into Eq. (17), we reach the following ODE:

$$\begin{aligned}&(c-2b_1b_2-b_1^2)\Phi'+\Phi'''+2\rho(\Phi^3)'\\&\quad+i\left(\left(b_3-b_1^2b_2\right)\Phi+(2b_1+b_2)\Phi''\right.\\&\quad\left.+2\rho(2b_1+b_2)\Phi^3\right)=0.\end{aligned} \tag{21}$$

The prime above denotes the derivative concerning ξ. Now, separating imaginary and real parts of Eq. (21), we reach

$$\begin{aligned}&(c-2b_1b_2-b_1^2)\Phi'+\Phi'''\\&\quad+2\rho(\Phi^3)'=0,\end{aligned} \tag{22}$$

$$\frac{\left(b_3-b_1^2b_2\right)}{(2b_1+b_2)}\Phi+\Phi''+2\rho\Phi^3=0. \tag{23}$$

By calculating the anti-derivative of Eq. (22) once, concerning ξ, and setting the integration constant to zero, we arrive at

$$(c-2b_1b_2-b_1^2)\Phi+\Phi''+2\rho\Phi^3=0. \tag{24}$$

Only in the event that the constraint condition is met are the Eqs. (23) and (24) equal

$$c-2b_1b_2-b_1^2=\frac{\left(b_3-b_1^2b_2\right)}{(2b_1+b_2)}. \tag{25}$$

Solving for

$$c=2b_1b_2+b_1^2+\frac{\left(b_3-b_1^2b_2\right)}{(2b_1+b_2)}, \tag{26}$$

we re-write Eq. (23) as:

$$\Phi''+\frac{\left(b_3-b_1^2b_2\right)}{(2b_1+b_2)}\Phi+2\rho\Phi^3=0. \tag{27}$$

4.1 Application of the nGERFM

Employing some common balancing rules in Eq. (27) between Φ^3 and Φ'' yields $3n_0=n_0+2$. Hence, one should take $n_0=1$. As a result, Eq. (8) can be written as:

$$\Phi(\xi)=k_0+k_1\left(\frac{\Lambda'(\xi)}{\Lambda(\xi)}\right)+l_1\left(\frac{\Lambda'(\xi)}{\Lambda(\xi)}\right)^{-1}. \tag{28}$$

$\Lambda(\xi)$ is defined by Eq. (9).

Class 1

Taking $[\varsigma_1,\varsigma_2,\varsigma_3,\varsigma_4]=[1,1,1,0]$ and $[\jmath_1,\jmath_2,\jmath_3,\jmath_4]=[0,1,2,0]$ in Eq. (9) yields

$$\Lambda(\xi)=\frac{1+\exp(\xi)}{\exp(2\xi)}. \tag{29}$$

To obtain parameter values, we use package programs (Maple or Mathematica) to solve algebraic equations. The set of answers that are produced can be provided as:

Type 1.1

$$b_1=\pm\frac{\mp1+\sqrt{1+4b_2b_3-2b_2^2}}{2b_2},$$

$$k_0=\mp\frac{5}{2}\sqrt{-\frac{1}{\rho}},\quad k_1=\pm\sqrt{-\frac{1}{\rho}},\quad l_1=0.$$

By plugging the aforementioned values of k_0, k_1, l_1 into Eq. (28), we obtain

$$\Phi^{\pm}(\xi) = \frac{1}{2}\sqrt{-\frac{1}{\rho}} \times \left(\frac{\exp(\xi)-1}{\exp(\xi)+1}\right). \tag{30}$$

By using Eq. (30), we discover the following exponential function solution for system (1)

$$\psi^{\pm}_{1,1}(x,y,t) = \frac{1}{2}\sqrt{-\frac{1}{\rho}} \times \left(\frac{\exp(x+y+ct)-1}{\exp(x+y+ct)+1}\right) \times \exp(i(\pm\frac{\mp 1+\sqrt{1+4b_2b_3-2b_2^2}}{2b_2}x + b_2y + b_3t)), \tag{31}$$

$$\varphi^{\pm}_{1,1}(x,y,t) = 2\rho(b_2 \pm \frac{\mp 1+\sqrt{1+4b_2b_3-2b_2^2}}{2b_2}) \times \left[\frac{1}{2}\sqrt{-\frac{1}{\rho}} \times \left(\frac{\exp(x+y+ct)-1}{\exp(x+y+ct)+1}\right)\right]^2, \tag{32}$$

$$\tau^{\pm}_{1,1}(x,y,t) = 2\rho \times \left[\frac{1}{2}\sqrt{-\frac{1}{\rho}} \times \left(\frac{\exp(x+y+ct)-1}{\exp(x+y+ct)+1}\right)\right]^2. \tag{33}$$

Type 1.2

$$b_1 = \pm\frac{\mp 1+\sqrt{1+4b_2b_3-2b_2^2}}{2b_2},$$

$$k_0 = \mp\frac{5}{2}\sqrt{-\frac{1}{\rho}}, \qquad k_1 = 0, \qquad l_1 = \pm 6\sqrt{-\frac{1}{\rho}}.$$

By inserting the aforementioned values of k_0, k_1, l_1 into Eq. (28), we get

$$\Phi^{\mp}(\xi) = \frac{1}{2}\sqrt{-\frac{1}{\rho}} \times \left(\frac{3\exp(\xi)-2}{3\exp(\xi)+2}\right). \tag{34}$$

Using Eq. (34), the exponential function solution is found for system (1) as follows:

$$\psi^{\mp}_{1,2}(x,y,t) = \frac{1}{2}\sqrt{-\frac{1}{\rho}} \times \left(\frac{3\exp(x+y+ct)-2}{3\exp(x+y+ct)+2}\right) \times \exp(i(\pm\frac{\mp 1+\sqrt{1+4b_2b_3-2b_2^2}}{2b_2}x + b_2y + b_3t)), \tag{35}$$

$$\varphi^{\mp}_{1,2}(x,y,t) = 2\rho(b_2 \pm \frac{\mp 1+\sqrt{1+4b_2b_3-2b_2^2}}{2b_2}) \times \left[\frac{1}{2}\sqrt{-\frac{1}{\rho}} \times \left(\frac{3\exp(x+y+ct)-2}{3\exp(x+y+ct)+2}\right)\right]^2, \tag{36}$$

$$\tau^{\mp}_{1,2}(x,y,t) = 2\rho \times \left[\frac{1}{2}\sqrt{-\frac{1}{\rho}} \times \left(\frac{3\exp(x+y+ct)-2}{3\exp(x+y+ct)+2}\right)\right]^2. \tag{37}$$

Class 2

When we pick $[\varsigma_1, \varsigma_2, \varsigma_3, \varsigma_4] = [1, -1, 2i, 0]$ and $[\jmath_1, \jmath_2, \jmath_3, \jmath_4] = [i, -i, 1, 0]$ in Eq. (9), we attain

$$\Lambda(\xi) = \frac{\sin(\xi)}{\exp(\xi)}. \tag{38}$$

Using package programs, we solve algebraic equations to acquire parameter values; the set of answers that arise can be provided as:

Type 2.1

$$b_1 = \pm\frac{\pm 2+\sqrt{4+b_2b_3+2b_2^2}}{b_2},$$

$$k_0 = k_1 = \pm\sqrt{-\frac{1}{\rho}}, \qquad l_1 = 0.$$

By plugging these values into Eq. (28), we yield

$$\Phi^{\pm}(\xi) = \sqrt{-\frac{1}{\rho}} \times \cot(\xi). \tag{39}$$

By using Eq. (39), we reach the following singular periodic optical soliton solution for system (1)

$$\psi^{\pm}_{2,1}(x,y,t) = \sqrt{-\frac{1}{\rho}} \times \cot(x+y+ct) \times \exp\left(i\left(\pm\frac{\pm 2+\sqrt{4+b_2b_3+2b_2^2}}{b_2}x + b_2y + b_3t\right)\right), \tag{40}$$

$$\varphi^{\pm}_{2,1}(x,y,t) = 2\rho\left(b_2 \pm \frac{\pm 2+\sqrt{4+b_2b_3+2b_2^2}}{b_2}\right) \times \left[\sqrt{-\frac{1}{\rho}} \times \cot(x+y+ct)\right]^2, \tag{41}$$

$$\tau^{\pm}_{2,1}(x,y,t) = 2\rho \times \left[\sqrt{-\frac{1}{\rho}} \times \cot(x+y+ct)\right]^2. \tag{42}$$

Type 2.2

$$b_1 = \pm\frac{\pm 2+\sqrt{4+b_2b_3+2b_2^2}}{b_2},$$

$$k_0 = \pm\sqrt{-\frac{1}{\rho}}, \qquad k_1 = 0, \qquad l_1 = \pm 2\sqrt{-\frac{1}{\rho}}.$$

By plugging these values into Eq. (28), we yield

$$\Phi^{\pm}(\xi)=\sqrt{-\frac{1}{\rho}}\times\left(\frac{\cos(\xi)+\sin(\xi)}{\cos(\xi)-\sin(\xi)}\right). \tag{43}$$

By using Eq. (43), the combo trigonometric soliton solution is obtained for system (1) as follows:

$$\begin{aligned}&\psi^{\pm}_{2,2}(x,y,t)\\&=\sqrt{-\frac{1}{\rho}}\times\left(\frac{\cos(x+y+ct)+\sin(x+y+ct)}{\cos(x+y+ct)-\sin(x+y+ct)}\right)\\&\quad\times\exp(i(\pm\frac{\pm2+\sqrt{4+b_2b_3+2b_2^2}}{b_2}x+b_2y+b_3t)),\end{aligned} \tag{44}$$

$$\begin{aligned}&\varphi^{\pm}_{2,2}(x,y,t)=2\rho(b_2\pm\frac{\pm2+\sqrt{4+b_2b_3+2b_2^2}}{b_2})\\&\quad\times\left[\sqrt{-\frac{1}{\rho}}\times\left(\frac{\cos(x+y+ct)+\sin(x+y+ct)}{\cos(x+y+ct)-\sin(x+y+ct)}\right)\right]^2,\end{aligned} \tag{45}$$

$$\begin{aligned}&\tau^{\pm}_{2,2}(x,y,t)=2\rho\\&\quad\times\left[\sqrt{-\frac{1}{\rho}}\times\left(\frac{\cos(x+y+ct)+\sin(x+y+ct)}{\cos(x+y+ct)-\sin(x+y+ct)}\right)\right]^2.\end{aligned} \tag{46}$$

Class 3

For $[\varsigma_1,\varsigma_2,\varsigma_3,\varsigma_4]=[1,-1,2,0]$ and $[\jmath_1,\jmath_2,\jmath_3,\jmath_4]=[1,-1,-1,0]$ in Eq. (9) provides

$$\Lambda(\xi)=\frac{\sinh(\xi)}{\exp(-\xi)}. \tag{47}$$

Proceeding as *the outline of nGERFM*, we achieve

$$b_1=\pm\frac{\mp2+\sqrt{4+b_2b_3-2b_2^2}}{b_2},$$

$$k_0=k_1=\pm\sqrt{-\frac{1}{\rho}},\qquad l_1=0.$$

By plugging these values into Eq. (28), we yield

$$\Phi^{\mp}(\xi)=\sqrt{-\frac{1}{\rho}}\times\tanh(\xi). \tag{48}$$

By using Eq. (48), we obtain the following shock wave solution for system (1)

$$\begin{aligned}&\psi^{\mp}_3(x,y,t)=\sqrt{-\frac{1}{\rho}}\times\tanh(x+y+ct)\\&\quad\times\exp\left(i\left(\pm\frac{\mp2+\sqrt{4+b_2b_3-2b_2^2}}{b_2}x+b_2y+b_3t\right)\right),\end{aligned} \tag{49}$$

$$\begin{aligned}&\varphi^{\mp}_3(x,y,t)=2\rho\left(b_2\pm\frac{\mp2+\sqrt{4+b_2b_3-2b_2^2}}{b_2}\right)\\&\quad\times\left[\sqrt{-\frac{1}{\rho}}\times\tanh(x+y+ct)\right]^2,\end{aligned} \tag{50}$$

$$\tau^{\mp}_3(x,y,t)=2\rho\times\left[\sqrt{-\frac{1}{\rho}}\times\tanh(x+y+ct)\right]^2. \tag{51}$$

Class 4

In Eq. (9), picking $[\varsigma_1,\varsigma_2,\varsigma_3,\varsigma_4]=[2,0,1,1]$ and $[\jmath_1,\jmath_2,\jmath_3,\jmath_4]=[1,0,i,-i]$ produces

$$\Lambda(\xi)=\frac{\exp(\xi)}{\cos(\xi)}. \tag{52}$$

We also arrive at

Type 4.1

$$b_1=\pm\frac{\pm2+\sqrt{4+b_2b_3+2b_2^2}}{b_2},$$

$$k_0=\mp\sqrt{-\frac{1}{\rho}},\qquad k_1=\pm\sqrt{-\frac{1}{\rho}},\qquad l_1=0.$$

Combining these results with Eq. (28) generates

$$\Phi^{\pm}(\xi)=\sqrt{-\frac{1}{\rho}}\times\tan(\xi). \tag{53}$$

As an outcome, we uncover that the singular periodic solution may be characterized as:

$$\begin{aligned}&\psi^{\pm}_{4,1}(x,y,t)=\sqrt{-\frac{1}{\rho}}\times\tan(x+y+ct)\\&\quad\times\exp\left(i\left(\pm\frac{\pm2+\sqrt{4+b_2b_3+2b_2^2}}{b_2}x+b_2y+b_3t\right)\right),\end{aligned} \tag{54}$$

$$\begin{aligned}&\varphi^{\pm}_{4,1}(x,y,t)=2\rho\left(b_2\pm\frac{\pm2+\sqrt{4+b_2b_3+2b_2^2}}{b_2}\right)\\&\quad\times\left[\sqrt{-\frac{1}{\rho}}\times\tan(x+y+ct)\right]^2,\end{aligned} \tag{55}$$

$$\tau^{\pm}_{4,1}(x,y,t)=2\rho\times\left[\sqrt{-\frac{1}{\rho}}\times\tan(x+y+ct)\right]^2. \tag{56}$$

Type 4.2

$$b_1=\pm\frac{\pm2+\sqrt{4+b_2b_3+2b_2^2}}{b_2},$$

$$k_0 = \pm\sqrt{-\frac{1}{\rho}}, \qquad k_1 = 0, \qquad l_1 = \mp 2\sqrt{-\frac{1}{\rho}}.$$

Combining these results with Eq. (28) produces

$$\Phi^{\pm}(\xi) = \sqrt{-\frac{1}{\rho}} \times \left(\frac{2\cos(\xi)\sin(\xi) - 1}{2\cos(\xi)^2 - 1}\right). \tag{57}$$

As a result, the combo trigonometric soliton solution is obtained as follows:

$$\psi^{\pm}_{4,2}(x, y, t) = \sqrt{-\frac{1}{\rho}} \times \left(\frac{2\cos(x+y+ct)\sin(x+y+ct) - 1}{2\cos(x+y+ct)^2 - 1}\right) \times \exp\left(i\left(\pm\frac{\pm 2 + \sqrt{4 + b_2 b_3 + 2b_2^2}}{b_2}x + b_2 y + b_3 t\right)\right), \tag{58}$$

$$\varphi^{\pm}_{4,2}(x, y, t) = 2\rho\left(b_2 \pm \frac{\pm 2 + \sqrt{4 + b_2 b_3 + 2b_2^2}}{b_2}\right) \times \left[\sqrt{-\frac{1}{\rho}} \times \left(\frac{2\cos(x+y+ct)\sin(x+y+ct) - 1}{2\cos(x+y+ct)^2 - 1}\right)\right]^2, \tag{59}$$

$$\tau^{\pm}_{4,2}(x, y, t) = 2\rho \times \left[\sqrt{-\frac{1}{\rho}} \times \left(\frac{2\cos(x+y+ct)\sin(x+y+ct) - 1}{2\cos(x+y+ct)^2 - 1}\right)\right]^2. \tag{60}$$

Class 5

In Eq. (9), considering $[\varsigma_1, \varsigma_2, \varsigma_3, \varsigma_4] = [2, 0, 1, 1]$ and $[J_1, J_2, J_3, J_4] = [0, 0, 1, -1]$ create

$$\Lambda(\xi) = \frac{1}{\cosh(\xi)}. \tag{61}$$

We accomplish

Type 5.1

$$b_1 = \pm\frac{\mp 2 + \sqrt{4 + b_2 b_3 - 2b_2^2}}{b_2},$$

$$k_0 = k_1 = 0, \qquad l_1 = \pm\sqrt{-\frac{1}{\rho}}.$$

By plugging the values of k_0, k_1, l_1 into Eq. (28), we gain

$$\Phi^{\mp}(\xi) = \sqrt{-\frac{1}{\rho}} \times \coth(\xi). \tag{62}$$

Hence, we uncover the singular soliton solutions can be derived as:

$$\psi^{\mp}_{5,1}(x, y, t) = \sqrt{-\frac{1}{\rho}} \times \coth(x+y+ct) \times \exp\left(i\left(\pm\frac{\mp 2 + \sqrt{4 + b_2 b_3 - 2b_2^2}}{b_2}x + b_2 y + b_3 t\right)\right), \tag{63}$$

$$\varphi^{\mp}_{5,1}(x, y, t) = 2\rho\left(b_2 \pm \frac{\mp 2 + \sqrt{4 + b_2 b_3 - 2b_2^2}}{b_2}\right) \times \left[\sqrt{-\frac{1}{\rho}} \times \coth(x+y+ct)\right]^2, \tag{64}$$

$$\tau^{\mp}_{5,1}(x, y, t) = 2\rho \times \left[\sqrt{-\frac{1}{\rho}} \times \coth(x+y+ct)\right]^2. \tag{65}$$

Type 5.2

$$b_1 = \pm\frac{\mp 8 + \sqrt{64 + b_2 b_3 - 8b_2^2}}{b_2},$$

$$k_0 = 0, \qquad k_1 = l_1 = \pm\sqrt{-\frac{1}{\rho}}.$$

Thus, concerning these solutions and Eq. (28), it is likely to reach the subsequent outcome

$$\Phi^{\mp}(\xi) = \sqrt{-\frac{1}{\rho}} \times \left(\frac{2\cosh(\xi)^2 - 1}{\cosh(\xi)\sinh(\xi)}\right). \tag{66}$$

The hyperbolic solution in mixed form may be stated as follows:

$$\psi^{\mp}_{5,2}(x, y, t) = \sqrt{-\frac{1}{\rho}} \times \left(\frac{2\cosh(x+y+ct)^2 - 1}{\cosh(x+y+ct)\sinh(x+y+ct)}\right) \times \exp\left(i\left(\pm\frac{\mp 8 + \sqrt{64 + b_2 b_3 - 8b_2^2}}{b_2}x + b_2 y + b_3 t\right)\right), \tag{67}$$

$$\varphi^{\mp}_{5,2}(x, y, t) = 2\rho\left(b_2 \pm \frac{\mp 8 + \sqrt{64 + b_2 b_3 - 8b_2^2}}{b_2}\right) \times \left[\sqrt{-\frac{1}{\rho}} \times \left(\frac{2\cosh(x+y+ct)^2 - 1}{\cosh(x+y+ct)\sinh(x+y+ct)}\right)\right]^2, \tag{68}$$

$$\tau^{\mp}_{5,2}(x, y, t) = 2\rho$$

$$\times\left[\sqrt{-\frac{1}{\rho}}\times\left(\frac{2\cosh(x+y+ct)^2-1}{\cosh(x+y+ct)\sinh(x+y+ct)}\right)\right]^2. \tag{69}$$

Class 6

As long as, and if it is taken into account in Eq. (9), $[\varsigma_1,\varsigma_2,\varsigma_3,\varsigma_4]=[2,0,1,1]$ and $[\jmath_1,\jmath_2,\jmath_3,\jmath_4]=[-2,0,1,-1]$ generates

$$\Lambda(\xi)=\frac{\exp(-2\xi)}{\cosh(\xi)}. \tag{70}$$

Type 6.1

$$b_1=\pm\frac{\mp2+\sqrt{4+b_2b_3-2b_2^2}}{b_2},$$

$$k_0=\mp\frac{2}{\rho\sqrt{-\frac{1}{\rho}}},\qquad k_1=\pm\sqrt{-\frac{1}{\rho}},\qquad l_1=0.$$

By entering the values of k_0,k_1,l_1 into Eq. (28), one obtains

$$\Phi^{\pm}(\xi)=\frac{1}{\rho\sqrt{-\frac{1}{\rho}}}\times\tanh(\xi). \tag{71}$$

By using Eq. (71), we recovered the following shock wave solutions

$$\psi^{\pm}_{6,1}(x,y,t)=\frac{1}{\rho\sqrt{-\frac{1}{\rho}}}\times\tanh(x+y+ct)\times\exp\left(i\left(\pm\frac{\mp2+\sqrt{4+b_2b_3-2b_2^2}}{b_2}x+b_2y+b_3t\right)\right), \tag{72}$$

$$\varphi^{\pm}_{6,1}(x,y,t)=2\rho\left(b_2\pm\frac{\mp2+\sqrt{4+b_2b_3-2b_2^2}}{b_2}\right)\times\left[\frac{1}{\rho\sqrt{-\frac{1}{\rho}}}\times\tanh(x+y+ct)\right]^2, \tag{73}$$

$$\tau^{\pm}_{6,1}(x,y,t)=2\rho\times\left[\frac{1}{\rho\sqrt{-\frac{1}{\rho}}}\times\tanh(x+y+ct)\right]^2. \tag{74}$$

Type 6.2

$$b_1=\pm\frac{\mp2+\sqrt{4+b_2b_3-2b_2^2}}{b_2},$$

$$k_0=\pm2\sqrt{-\frac{1}{\rho}},\qquad k_1=0,\qquad l_1=\pm3\sqrt{-\frac{1}{\rho}}.$$

By entering the values of k_0,k_1,l_1 into Eq. (28), one obtains

$$\Phi^{\pm}(\xi)=\sqrt{-\frac{1}{\rho}}\times\left(\frac{2\sinh(\xi)+\cosh(\xi)}{2\cosh(\xi)+\sinh(\xi)}\right). \tag{75}$$

By using Eq. (75), we reach the combo soliton solution

$$\psi^{\pm}_{6,2}(x,y,t)=\sqrt{-\frac{1}{\rho}}\times\left(\frac{2\sinh(x+y+ct)+\cosh(x+y+ct)}{2\cosh(x+y+ct)+\sinh(x+y+ct)}\right)\times\exp\left(i\left(\pm\frac{\mp2+\sqrt{4+b_2b_3-2b_2^2}}{b_2}x+b_2y+b_3t\right)\right), \tag{76}$$

$$\varphi^{\pm}_{6,2}(x,y,t)=2\rho\left(b_2\pm\frac{\mp2+\sqrt{4+b_2b_3-2b_2^2}}{b_2}\right)\times\left[\sqrt{-\frac{1}{\rho}}\times\left(\frac{\cosh(x+y+ct)+2\sinh(x+y+ct)}{2\cosh(x+y+ct)+\sinh(x+y+ct)}\right)\right]^2, \tag{77}$$

$$\tau^{\pm}_{6,2}(x,y,t)=2\rho\times\left[\sqrt{-\frac{1}{\rho}}\times\left(\frac{\cosh(x+y+ct)+2\sinh(x+y+ct)}{2\cosh(x+y+ct)+\sinh(x+y+ct)}\right)\right]^2. \tag{78}$$

Class 7

If we take $[\varsigma_1,\varsigma_2,\varsigma_3,\varsigma_4]=[1,1,2,0]$ and $[\jmath_1,\jmath_2,\jmath_3,\jmath_4]=[i,-i,0,0]$ in Eq. (9) offers

$$\Lambda(\xi)=\cos(\xi). \tag{79}$$

We have,

$$b_1=\pm\frac{\mp4+\sqrt{16+b_2b_3-4b_2^2}}{b_2},$$

$$k_0=0,\qquad k_1=l_1=\pm\sqrt{-\frac{1}{\rho}}.$$

If these outcomes are taken into account along with Eq. (28), the next result is got

$$\Phi^{\mp}(\xi)=\sqrt{-\frac{1}{\rho}}\times\frac{1}{\cos(\xi)\sin(\xi)}. \tag{80}$$

Thus, we have the following periodic solution

$$\psi^{\mp}_{7}(x,y,t)=\sqrt{-\frac{1}{\rho}}\times\frac{1}{\cos(x+y+ct)\sin(x+y+ct)}$$

$$\times \exp\left(i\left(\pm\frac{\mp 4+\sqrt{16+b_2b_3-4b_2^2}}{b_2}x+b_2y+b_3t\right)\right), \tag{81}$$

$$\varphi_7^{\mp}(x,y,t)=2\rho\left(b_2\pm\frac{\mp 4+\sqrt{16+b_2b_3-4b_2^2}}{b_2}\right)\times\left[\sqrt{-\frac{1}{\rho}}\times\frac{1}{\sin(x+y+ct)\cos(x+y+ct)}\right]^2, \tag{82}$$

$$\tau_7^{\mp}(x,y,t)=2\rho\times\left[\sqrt{-\frac{1}{\rho}}\times\frac{1}{\sin(x+y+ct)\cos(x+y+ct)}\right]^2. \tag{83}$$

5 Qualitative analysis

This section provides a thorough examination of the governing equation's bifurcation analysis, sensitivity analysis, quasi-periodic and chaotic behaviors, and multistability analysis.

5.1 Bifurcation analysis

Depending on the equilibrium points, phase pictures of dynamical systems can undergo considerable changes. The phase image of a dynamical system implies a wave solution for the underlying nonlinear equation for each orbit. The study of nonlinear dynamics relies heavily on the bifurcation theory of planar dynamical systems (PDSs) [35–39].

Equation (27) defined as:

$$\Phi''+\frac{(b_3-b_1^2b_2)}{(2b_1+b_2)}\Phi+2\rho\Phi^3=0.$$

Let's modify the above equation to make things simpler

$$\Phi''+\varpi_1\Phi^3+\varpi_2\Phi=0, \tag{84}$$

in which $2\rho=\varpi_1$, and $\frac{(b_3-b_1^2b_2)}{(2b_1+b_2)}=\varpi_2$.

Denote $\Phi'=T$ in Eq. (84) to obtain the PDS, which is as follows:

$$\begin{cases}\frac{d\Phi}{d\xi}=T,\\ \frac{dT}{d\xi}=-\varpi_1\Phi^3-\varpi_2\Phi.\end{cases} \tag{85}$$

The roots of $-\varpi_1\Phi^3-\varpi_2\Phi$ are the equilibrium points (EPs) on the axis $T=0$ that correspond to the PDS (85). The obtained result is

$$g(\Phi)=-\varpi_1\Phi^3-\varpi_2\Phi. \tag{86}$$

Consequently, the aforementioned system (85) has unique EP $\Upsilon_1=(0,0)$ if $\varpi_1\varpi_2>0$ also $\varpi_1\varpi_2<0$ then, (85) contains these EPs: $\Upsilon_1=(0,0)$, $\Upsilon_2=\left(\sqrt{-\frac{\varpi_2}{\varpi_1}},0\right)$, and $\Upsilon_3=\left(-\sqrt{-\frac{\varpi_2}{\varpi_1}},0\right)$.

Let $W(\Phi,T)$ represent the *linearized system's coefficient matrix* at EP (Φ,T). This matrix is referred to as the system's "Jacobian" matrix. The determinant of the Jacobian matrix, denoted by PDS (85), is expressed as:

$$det[J(\Phi,T)]=3\varpi_1\Phi^2+\varpi_2, \tag{87}$$

in which $(\Phi,0)$ is system's EP for (85). Based on the bifurcation theory, if $det[J(\Phi,0)]=0$, the EP of PDS (85) is a *cusp point, if* $det[J(\Phi,0)]<0$ the EP of (85) is a *saddle point, and if* $det[J(\Phi,0)]>0$ the EP of (85) is a *center point* along the Poincare index of the EP is zero. The bifurcation of the PDS depending on the parameters ϖ_1, and ϖ_2.

When we consider $\varpi_1>0$, $\varpi_2>0$ then, the center point of (85) is EP $\Upsilon_1=(0,0)$, since $det[J(\Phi,T)]>0$ in (87). If we choose $\varpi_1>0$, $\varpi_2<0$ then, (85) has three EPs: $\Upsilon_1=(0,0)$, $\Upsilon_2=\left(\sqrt{-\frac{\varpi_2}{\varpi_1}},0\right)$, and $\Upsilon_3=\left(-\sqrt{-\frac{\varpi_2}{\varpi_1}},0\right)$. Because of this, the Jacobi matrix's determinant for $\Upsilon_1=(0,0)$ is negative, suggesting that this point is the saddle. Moreover, this indicates that $\Upsilon_2=\left(\sqrt{-\frac{\varpi_2}{\varpi_1}},0\right)$, and $\Upsilon_3=\left(-\sqrt{-\frac{\varpi_2}{\varpi_1}},0\right)$ are center points because they are both positive. When we take $\varpi_1<0$, $\varpi_2>0$ then, (85) has three EPs: $\Upsilon_1=(0,0)$, $\Upsilon_2=\left(\sqrt{-\frac{\varpi_2}{\varpi_1}},0\right)$, and $\Upsilon_3=\left(-\sqrt{-\frac{\varpi_2}{\varpi_1}},0\right)$. Because of this, the center of $\Upsilon_1=(0,0)$ is indicated by the positive determinant of the Jacobi matrix. Additionally, $\Upsilon_2=\left(\sqrt{-\frac{\varpi_2}{\varpi_1}},0\right)$, $\Upsilon_3=\left(-\sqrt{-\frac{\varpi_2}{\varpi_1}},0\right)$ have negative Jacobi matrix determinants, suggesting that they are saddle. If we regard $\varpi_1<0$, $\varpi_2<0$ then, $\Upsilon_1=(0,0)$ is the only EP for (85), and it is classified as a saddle point due to the negative determinant of the Jacobi matrix in (87).

5.2 Sensitivity analysis

In this subsection, we operate the Runge–Kutta method to scrutinize the sensitivity of the dynamical system described by PDS (85) [40]. The PDS (85) is chosen for investigation in this subsection utilizing sensitivity inspections. Keeping the parameters as they are in Figs. 2, 3, 4 and 5, respectively, yields four non-

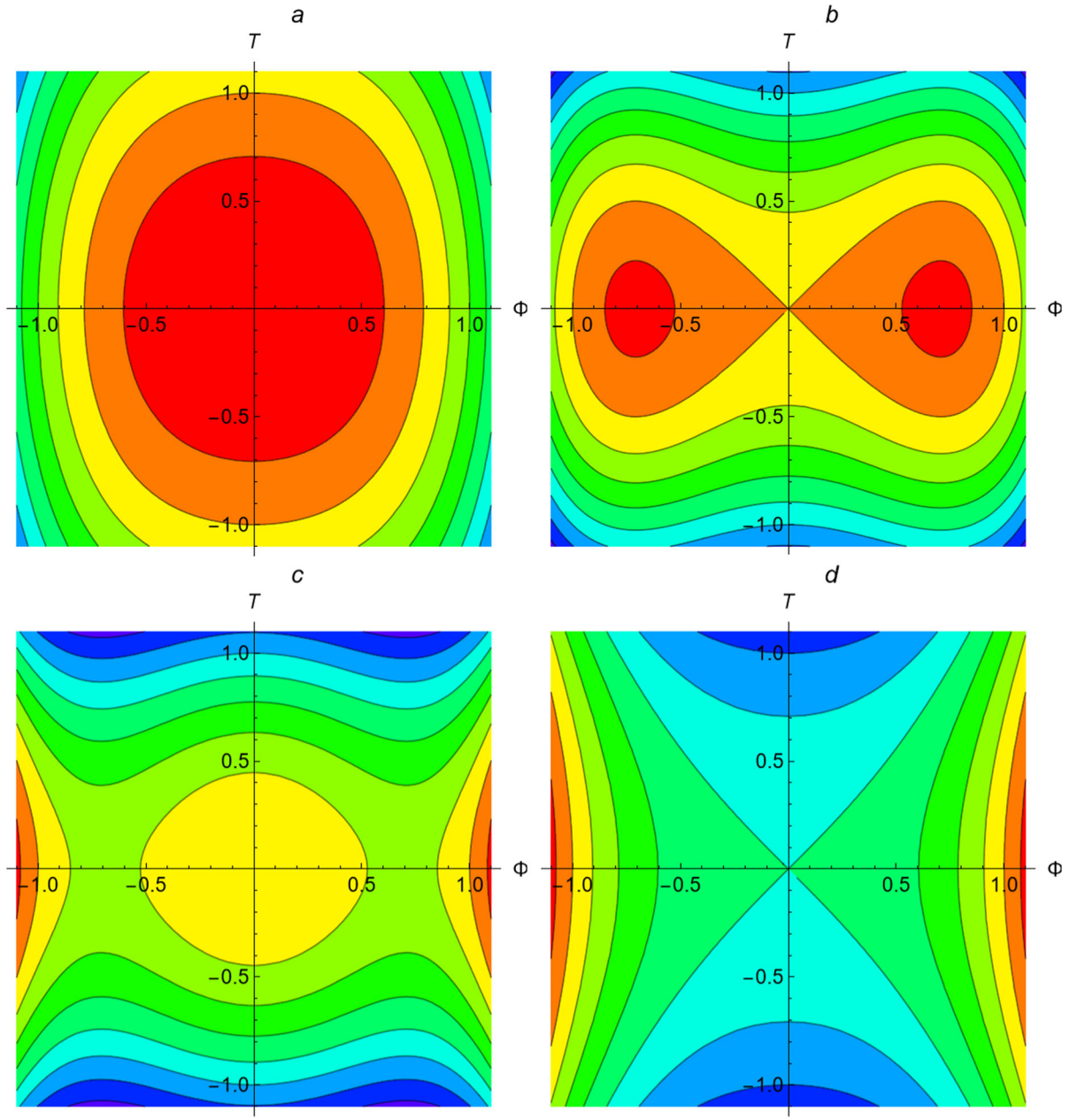


Fig. 1 Phase portraits for the system (85)

identical initial values. It may be shown that the PDS (85) exhibits a quasi-periodic pattern under the initial tested circumstances. It is evident from the figures that even minor modifications to the starting conditions result in significant shifts in the system's behavior. A comprehensive analysis of these graphical representations unmistakably reveals that even minor adjustments in the initial conditions yield significant disparities in the overall dynamics exhibited by the system. This phenomenon underscores the system's inherent sensitivity to its initial state, where even slight deviations can trigger substantial divergences in the subsequent trajectory and behavior.

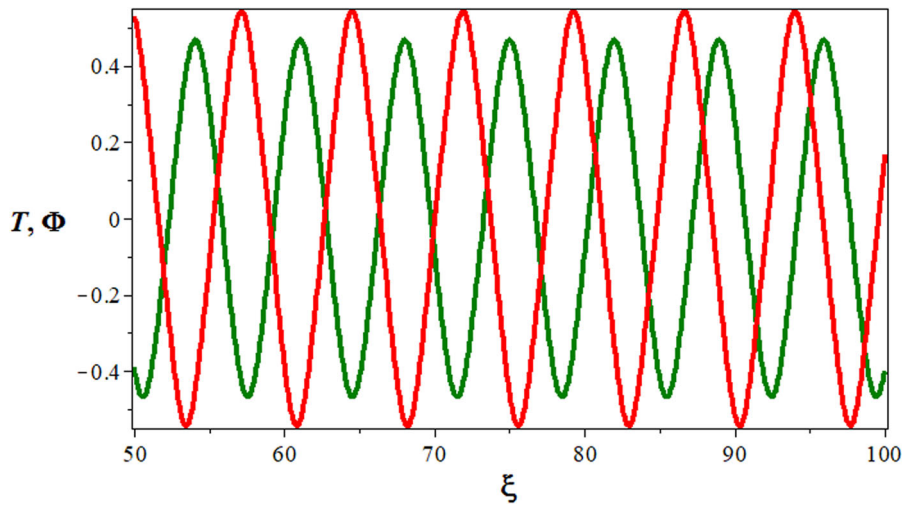


Fig. 2 Plot of the sensitivity of the dynamical structure (85) for $(\Phi(0), T(0)) = (0.6, 0.0)$ in the red hue, $(\Phi(0), T(0)) = (0.5, 0.0)$ in the green hue, for $\varpi_1 = -1$, $\varpi_2 = 1$ when $b_1 = 2$, $b_2 = -2$, $b_3 = -6$, $\rho = \frac{1}{2}$, and stepsize= 0.05

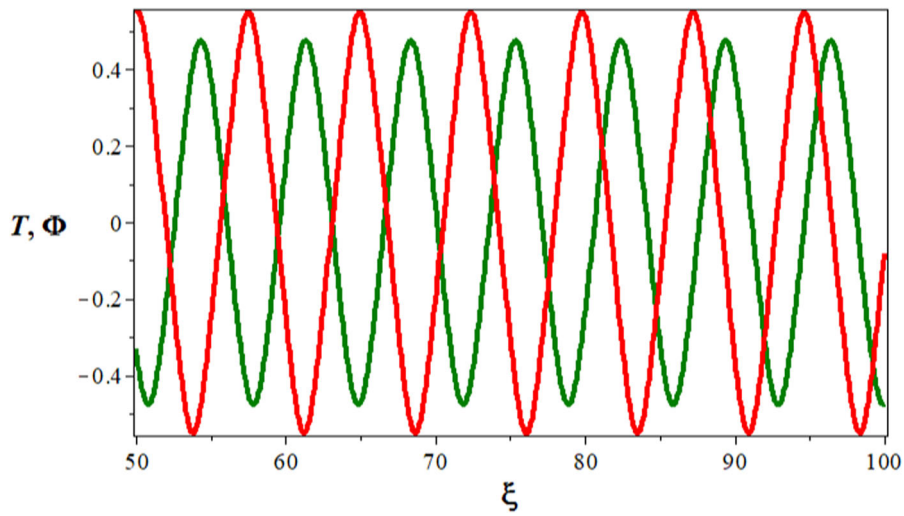


Fig. 3 Plot of the sensitivity of the dynamical structure (85) for $(\Phi(0), T(0)) = (0.61, 0.0)$ in the red hue, $(\Phi(0), T(0)) = (0.51, 0.0)$ in the green hue, for $\varpi_1 = -1$, $\varpi_2 = 1$ when $b_1 = 2$, $b_2 = -2$, $b_3 = -6$, $\rho = \frac{1}{2}$, and stepsize= 0.05

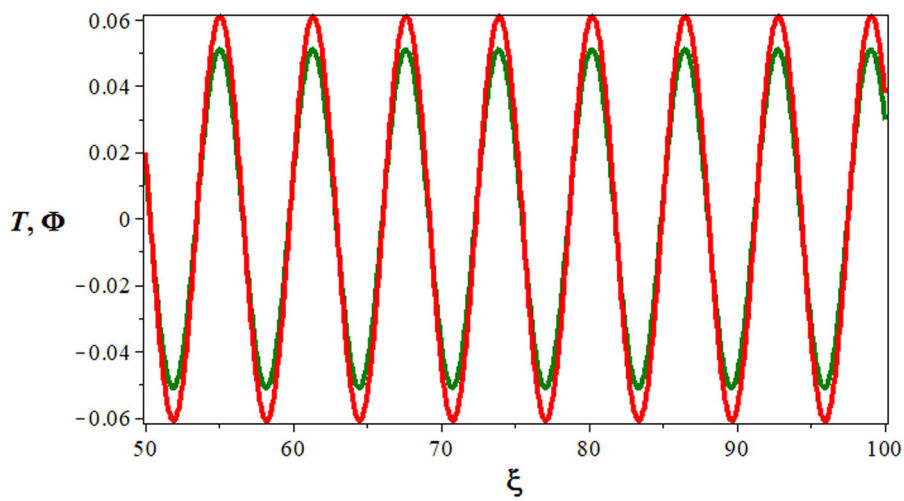


Fig. 4 Plot of the sensitivity of the dynamical structure (85) for $(\Phi(0), T(0)) = (0.061, 0.0)$ in the red hue, $(\Phi(0), T(0)) = (0.051, 0.0)$ in the green hue, for $\varpi_1 = -1$, $\varpi_2 = 1$ when $b_1 = 2$, $b_2 = -2$, $b_3 = -6$, $\rho = \frac{1}{2}$, and stepsize= 0.05

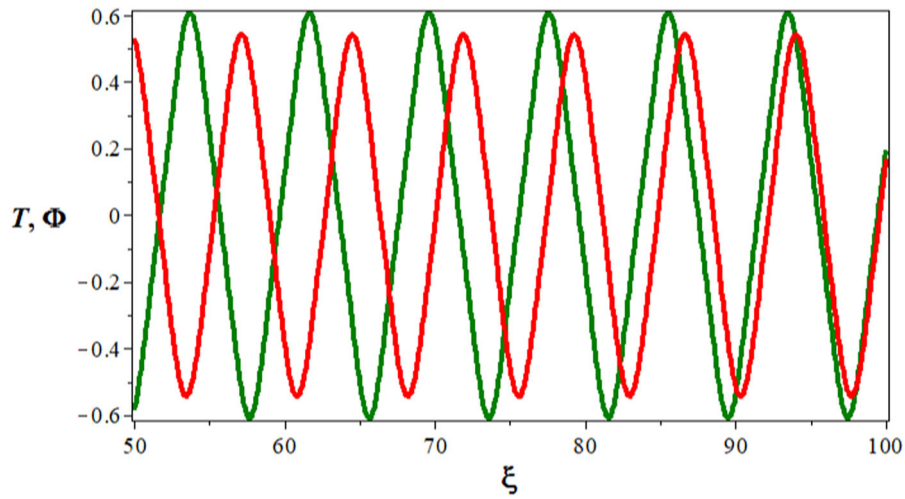


Fig. 5 Plot of the sensitivity of the dynamical structure (85) for $(\Phi(0), T(0)) = (0.6, 0.0)$ in the red hue, $(\Phi(0), T(0)) = (0.7, 0.0)$ in the green hue, for $\varpi_1 = -1$, $\varpi_2 = 1$ when $b_1 = 2$, $b_2 = -2$, $b_3 = -6$, $\rho = \frac{1}{2}$, and stepsize= 0.05

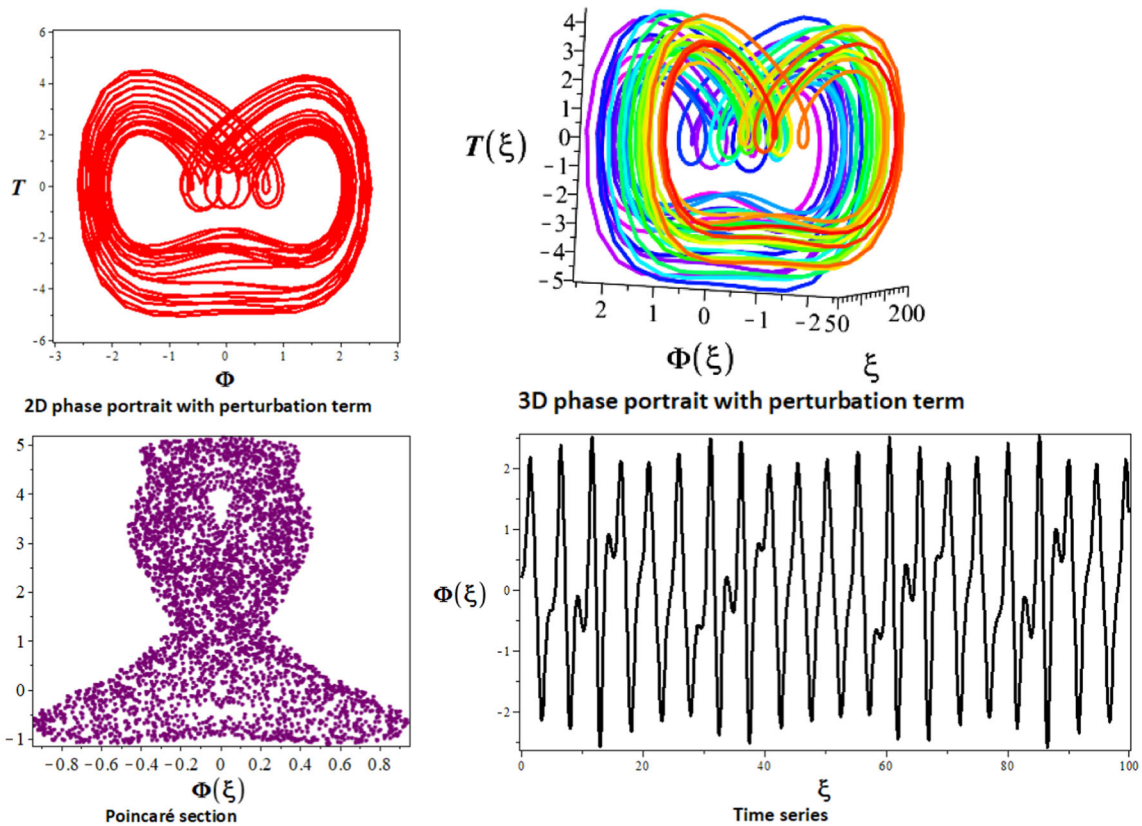


Fig. 6 The nonlinear dynamical system for $\varpi_1 = 1.5$, $\varpi_2 = 0.1$, $\epsilon = 5.1$, and $\varrho = 1.28$ with the initial condition $(\Phi(0), T(0)) = (0.20, 0.15)$ is shown, when $b_1 = 1$, $b_2 = 8$, $b_3 = 9$, $\rho = 3/4$

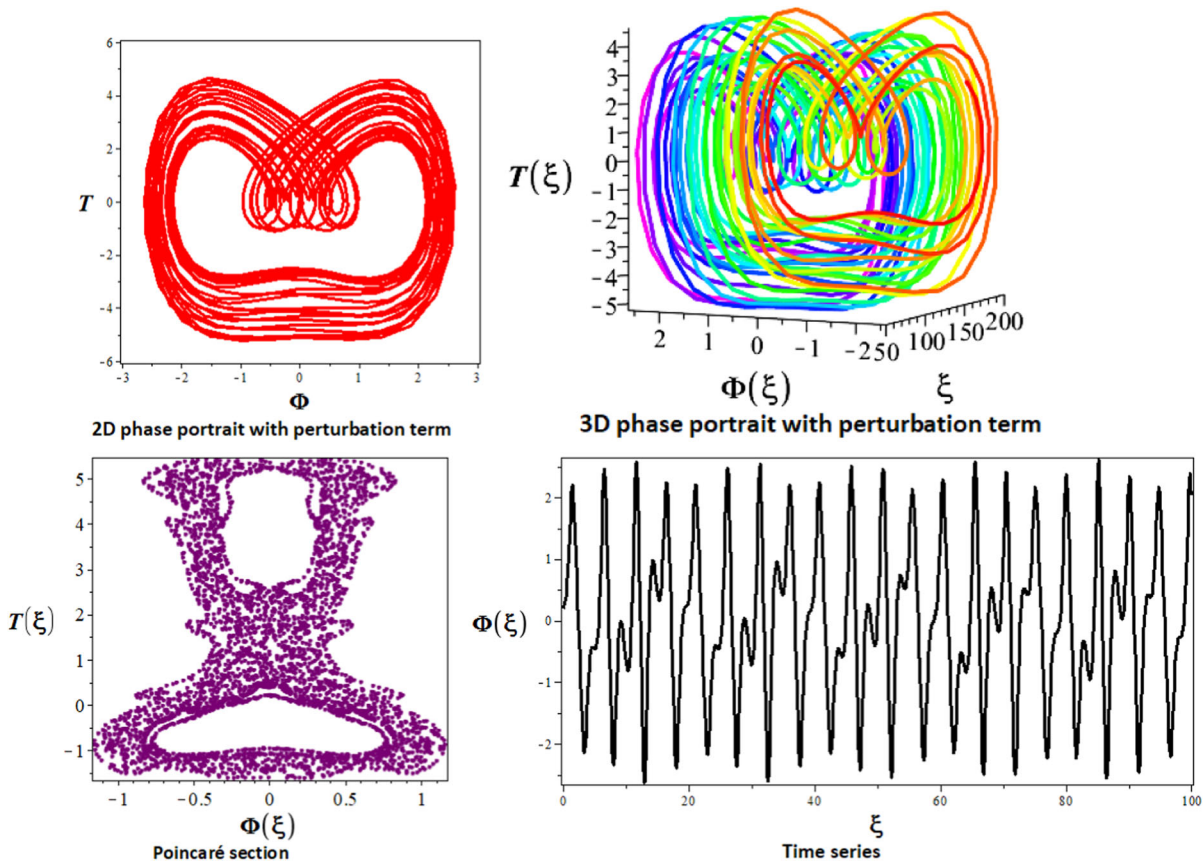


Fig. 7 The nonlinear dynamical system for $\varpi_1 = 1.5$, $\varpi_2 = 0.1$, $\epsilon = 5.3$, and $\varrho = 1.28$ with the initial condition $(\Phi(0), T(0)) = (0.20, 0.15)$ is shown

5.3 Quasi periodic and chaotic behaviors

By introducing the perturbation term ϱ, formulation (85) may be interpreted into the perturbed dynamical system (pDS) $\varrho \sin(\epsilon\xi)$:

$$\begin{cases} \frac{d\Phi}{d\xi} = T, \\ \frac{dT}{d\xi} = -\varpi_1\Phi^3 - \varpi_2\Phi + \varrho\sin(\epsilon\xi) \end{cases} \tag{88}$$

where ϱ and ϵ represent the magnitude and frequency of the external force exerted on the system (88). In this analysis, we will investigate how the factors ϱ and ϵ of the perturbation term effect the pDS (85). For this reason, we will fix all other physical parameters of the (88) and then observe the effects of ϱ and ϵ.

5.4 Multistability analysis

This subsection handles the multistability of a system like (88) for the perturbed term. To explore a dynamical system's tendency toward multistability (88), multistability [40–42] is the concurrent combination of numerous, even massive, solutions for a given range of physical variables and variable beginning values. For $\varpi_1 = 0.5$, $\varpi_2 = 0.1$ ($b_1 = 1$, $b_2 = 8$, $b_3 = 9$, and $\rho = 1/4$), $\varrho = 8.1$, $\epsilon = 8.923$, and stepsize$= 0.1$ two distinct phase portrait types can be created for the beginning conditions $(\Phi, T) = (1.8, 1.25)$ and $(\Phi, T) = (0.20, 0.15)$, which represents the hues red and black. A quasi-periodic style is detected in the beginning value $(1.8, 1.25)$ by the tested system, although the periodic style indicated a similar number of variables with the initial condition $(0.20, 0.15)$.

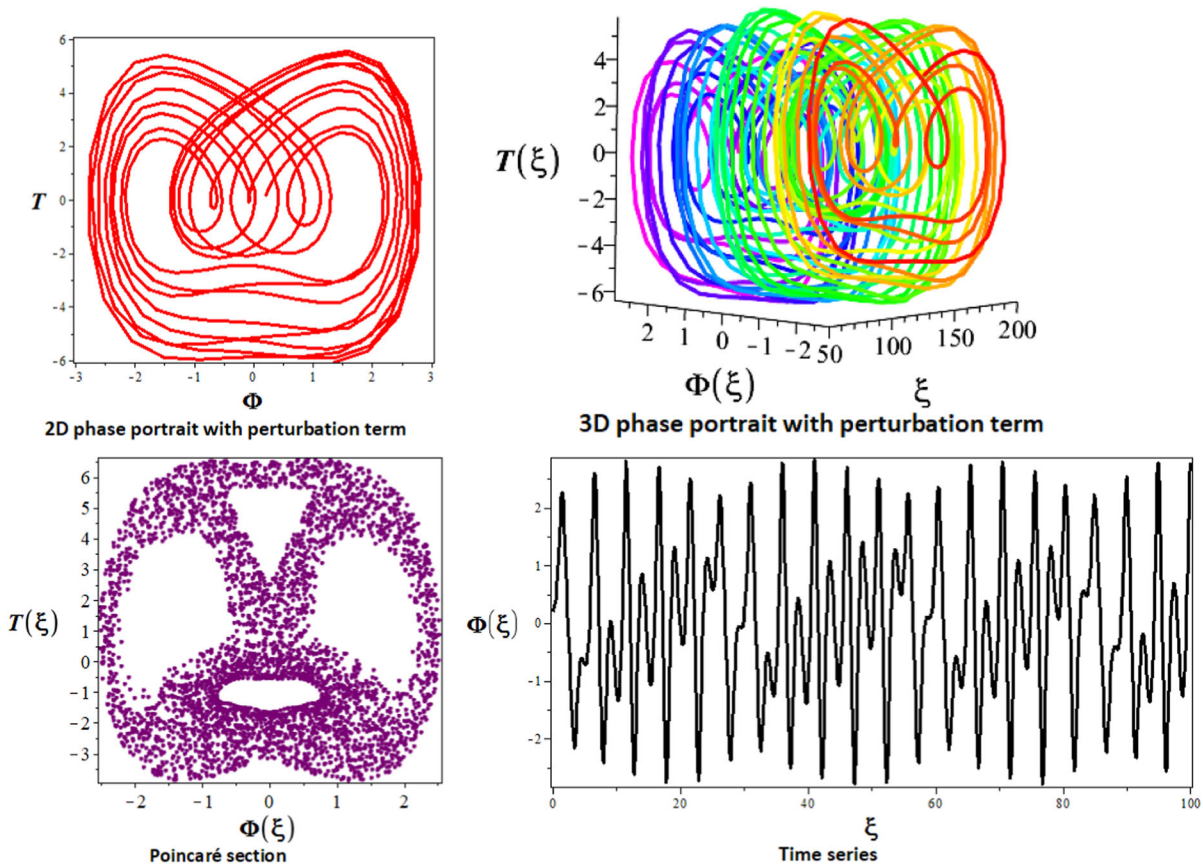


Fig. 8 The nonlinear dynamical system for $\varpi_1 = 1.5$, $\varpi_2 = 0.1$, $\epsilon = 5.8$, and $\varrho = 1.28$ with the initial condition $(\Phi(0), T(0)) = (0.20, 0.15)$ is shown

6 Comparisons

This section compares the results of this investigation with other studies that were acquired using different analytical techniques and published in the literature. The purpose of this comparative analysis is to draw attention to the distinctive features and novel contributions of the present study. In [28], the (2+1)-dimensional cmKdV system was studied by using the Darboux transformation to find soliton solutions. In [43], the author uncovered analytical solutions, including dark solitons, bright solitons, and periodic waves by using the the improved Sardar equation method. Our work synthesizes this research to apply the more effective technique, namely the nGERFM. Thus, by implementing the above methodology, we give novel soliton solutions, such as exponential function solutions, singular periodic wave solutions, combo trigonometric solutions, shock wave solutions, singular soliton solutions, and hyperbolic solutions in mixed form. Furthermore, the examination of bifurcation in the model mentioned above is explored, a crucial aspect in the study of dynamical systems. Chaos theory and bifurcation theory are essential instruments for comprehending intricate systems and are widely applicable in various scientific fields. This assessment plays a significant role in elucidating the resilience and enduring dynamics of solitons in diverse physical systems.

It becomes clear that several of the conclusions in this study, which were attained by carefully choosing the parameters, are consistent with findings from earlier research. It is important to remember that, despite possible similarities, the original expressions of these results are not the same as ours. Despite an extensive search of relevant publications, no solution identical to the one revealed in this work could be found. Because

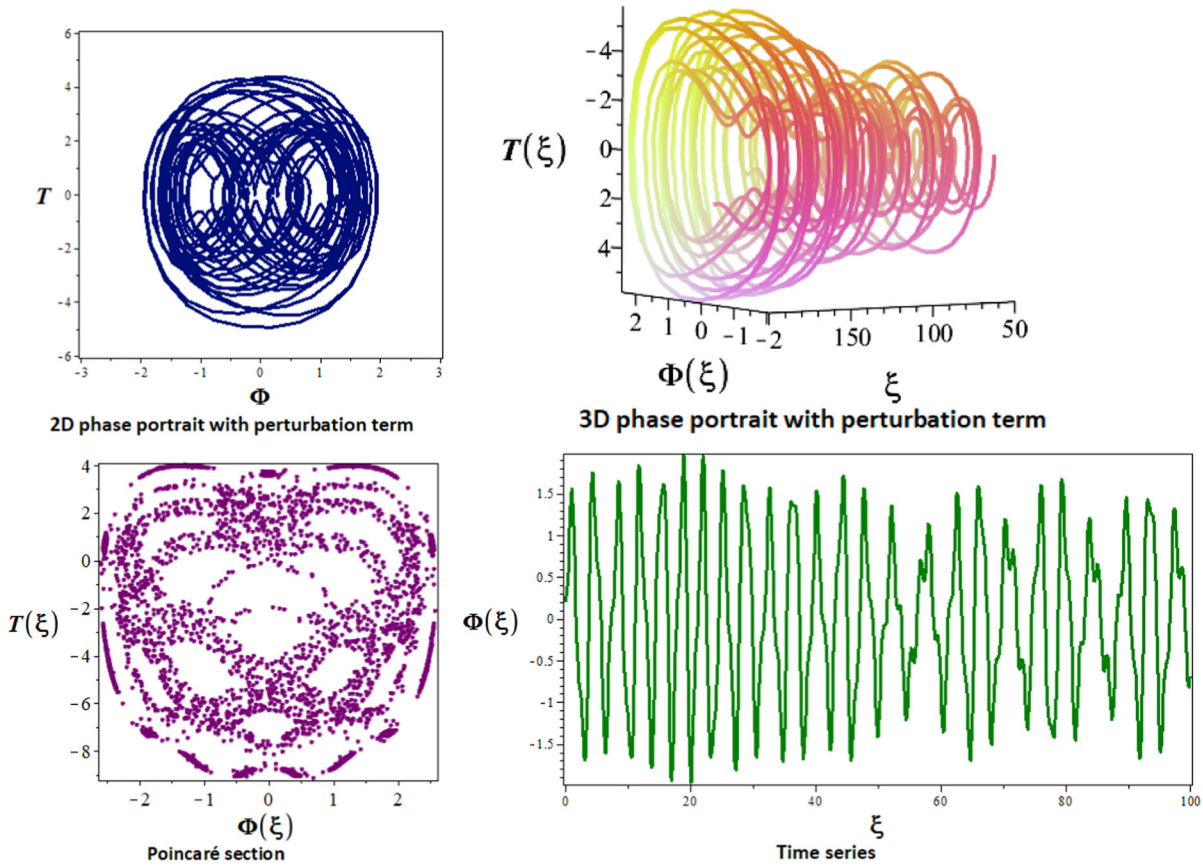


Fig. 9 The nonlinear dynamical system for $\varpi_1 = 1.5$, $\varpi_2 = 0.1$, $\epsilon = 5.1$, and $\varrho = 4.18$ with the initial condition $(\Phi(0), T(0)) = (0.20, 0.15)$ is shown

they do not seem to have been published before, it is notable that the remaining results we have obtained are new and inventive. The results presented in this research were obtained by applying the nGERFM. On the other hand, the retrieved results differ from the previous ones obtained by [33] as well.

7 Graphical explanation

This section showcases graphical representations of the obtained solutions. 3D, contour and density plots were created for some solutions obtained using the nGERFM. These graphs were generated using the Mathematica program by taking the absolute value of the obtained solutions. By using the Maple program, graphs for bifurcation analysis, sensitivity analysis, quasi-periodic and chaotic behaviors, and multistability analysis are also included.

For Fig. 1a shows the phase portrait for $\varpi_1 = 1$, $\varpi_2 = 1$ ($\varpi_1 > 0$, $\varpi_2 > 0$) when $b_1 = 2$, $b_2 = -2$, $b_3 = -6$, $\rho = \frac{1}{2}$.

For Fig. 1b depicts the phase graph for $\varpi_1 = 1$, $\varpi_2 = -1$ ($\varpi_1 > 0$, $\varpi_2 < 0$) when $b_1 = 2$, $b_2 = -2$, $b_3 = -10$, $\rho = \frac{1}{2}$.

For Fig. 1c illustrates the phase picture for $\varpi_1 = -1$, $\varpi_2 = 1$ ($\varpi_1 < 0$, $\varpi_2 > 0$) when $b_1 = 2$, $b_2 = -2$, $b_3 = -6$, $\rho = -\frac{1}{2}$.

For Fig. 1d demonstrates the phase image for $\varpi_1 = -1$, $\varpi_2 = -1$ ($\varpi_1 < 0$, $\varpi_2 < 0$) when $b_1 = 2$, $b_2 = -2$, $b_3 = -10$, $\rho = -\frac{1}{2}$.

In our simulations for Figs. 2, 3, 4, 5, 6, 7, 8, 9, 10, 11 and 12, we observe a variety of intricate and anomalous phenomena within natural systems. Upon examination of the graphical representations, it becomes evident that even minor alterations in initial conditions yield significant disruptions within the system, leading to the emer-

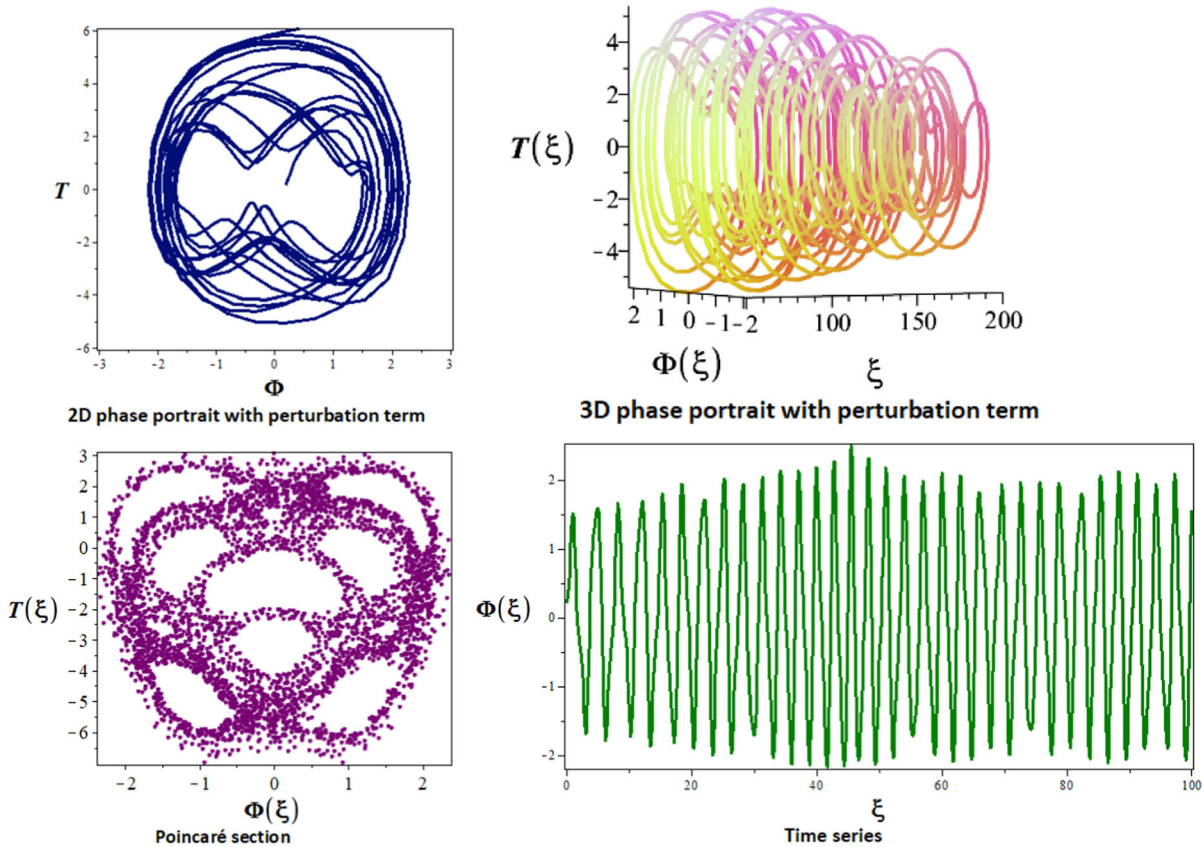


Fig. 10 The nonlinear dynamical system for $\varpi_1 = 1.5$, $\varpi_2 = 0.1$, $\epsilon = 5.1$, and $\varrho = 4.38$ with the initial condition $(\Phi(0), T(0)) = (0.20, 0.15)$ is shown

gence of novel and peculiar behaviors. These observations underscore the profound impact of slight modifications in the initial state, revealing a pronounced sensitivity of the system under scrutiny to its initial parameters. It is within the dynamic interplay between order and disorder that we witness the genesis of innovative phenomena, where minute perturbations can precipitate divergent outcomes on a grand scale. As we probe deeper into the realm of chaos, we encounter elusive attractors and fractal structures, which provide tantalizing glimpses of underlying stability amidst apparent randomness. The exploration of chaotic systems poses formidable challenges to conventional notions of predictability, necessitating the utilization of sophisticated mathematical methodologies to elucidate discernible patterns amidst the apparent disorder while embracing the enigmatic essence of these intricately intertwined systems (Figs. 13, 14, 15, 16, 17).

8 Conclusion

This paper considered the (2+1) dimensional cmKdV system. The cmKdV is a complex extension of the well-known Korteweg–de Vries (KdV) equation, which describes the propagation of long waves in shallow water.

To begin with, we regarded the nGERFM. Thanks to the nGERFM, we obtained various types of soliton solutions, such as exponential function solutions, singular periodic wave solutions, combo trigonometric solutions, shock wave solutions, singular soliton solutions, and hyperbolic solutions in mixed form. Predicted arrangements for solutions are established from the outset, which is one of these methodologies' major advantages. To visualize the graphical representation of the acquired soliton solutions, 3D, density, and contour curves were plotted by choosing suitable parameter values via Mathematica. The approach used is clear and

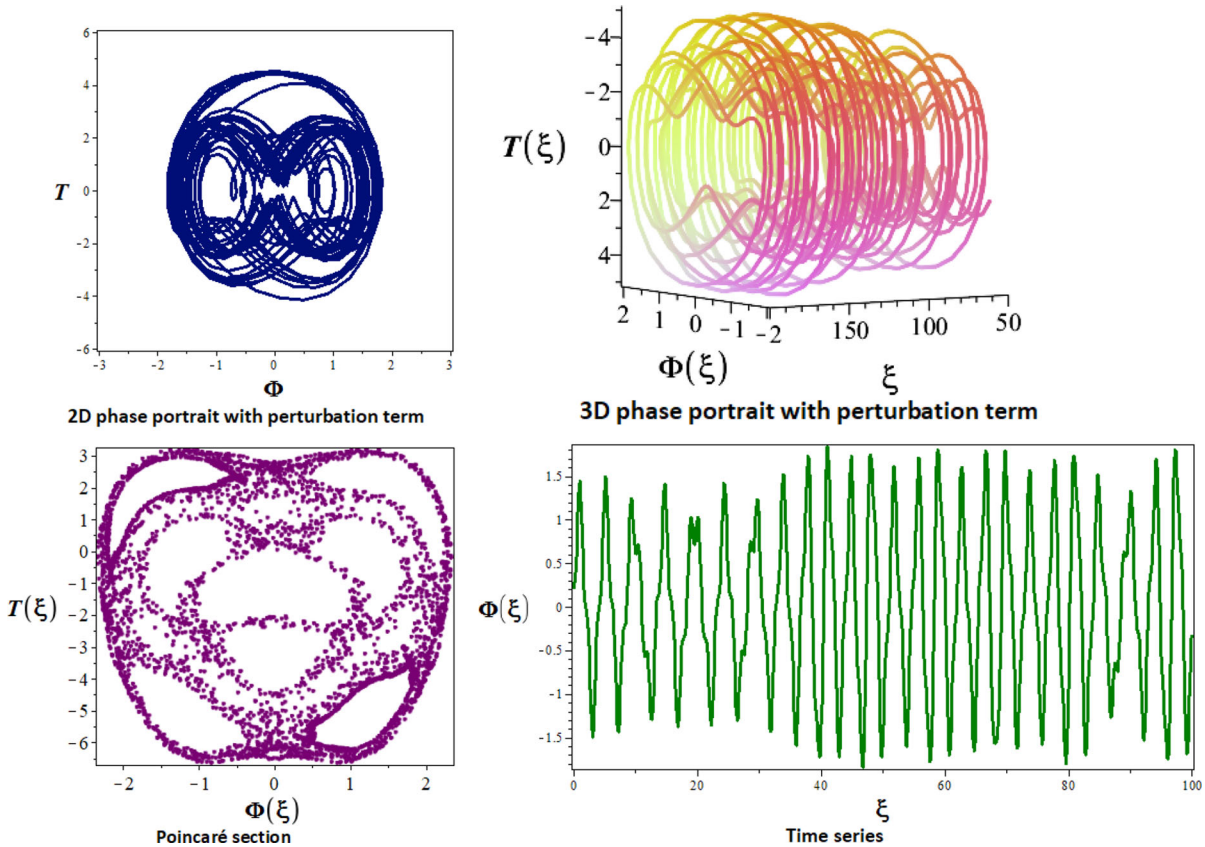


Fig. 11 The nonlinear dynamical system for $\varpi_1 = 1.5$, $\varpi_2 = 0.1$, $\epsilon = 5.1$, and $\varrho = 4.58$ with the initial condition $(\Phi(0), T(0)) = (0.20, 0.15)$ is shown

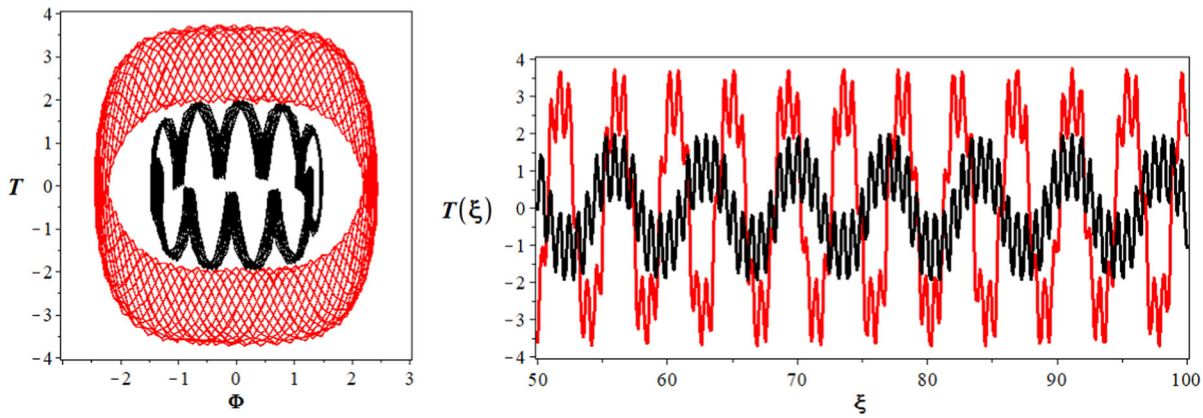


Fig. 12 Multistability of the dynamical system for $(\Phi, T) = (1.8, 1.25)$ in red hue, and $(\Phi, T) = (0.20, 0.15)$ in a black hue

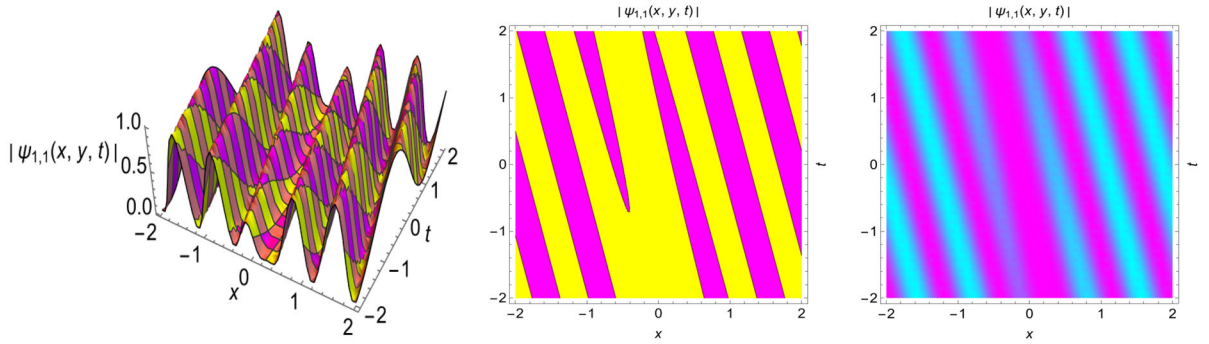


Fig. 13 The 3D, contour, and density plots for the solution $\left|\psi_{1,1}(x, y, t)\right|$ in (31) when $b_1 = 1$, $b_2 = 2$, $b_3 = 4$, $\rho = 2$, $c = 11/2$, and $y = 1$

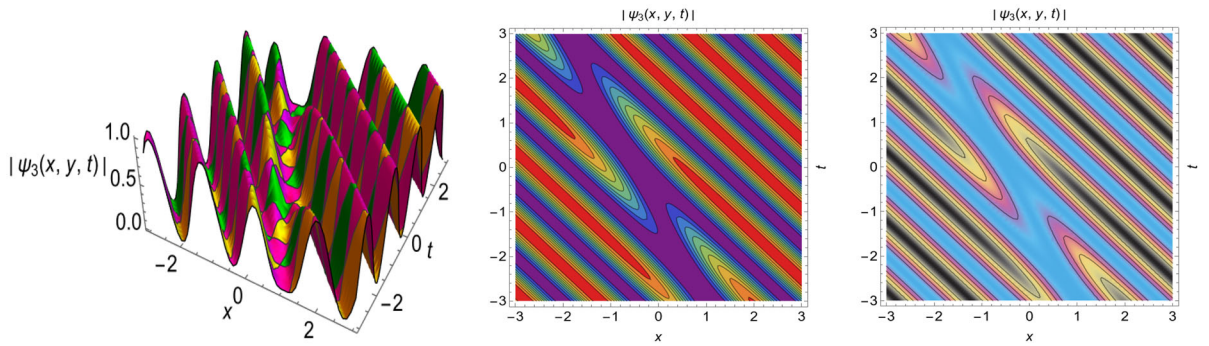


Fig. 14 The 3D, contour, and density plots for the solution $|\psi_3(x, y, t)|$ in (49) when $b_1 = -2$, $b_2 = 1$, $b_3 = -2$, $\rho = 2$, $c = 2$, and $y = 1$

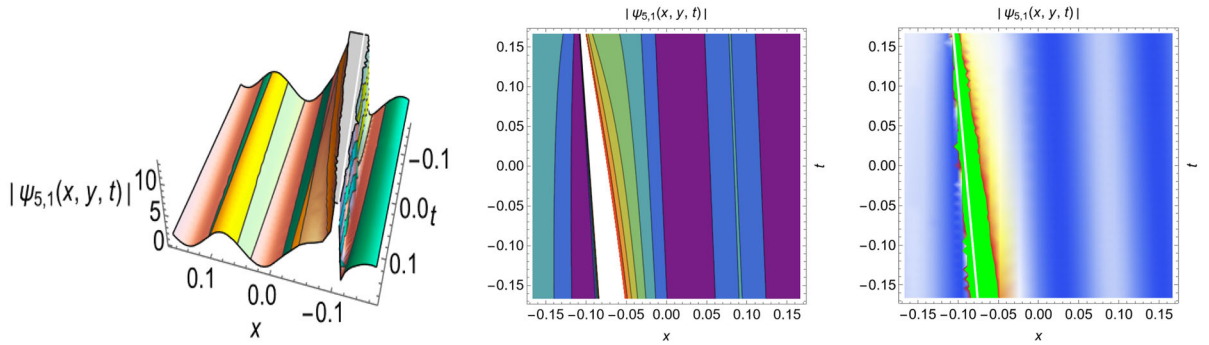


Fig. 15 The 3D, contour, and density plots for the solution $\left|\psi_{5,1}(x, y, t)\right|$ in (67) when $b_1 = 1$, $b_2 = 1$, $b_3 = 25$, $\rho = 2$, $c = 11$, and $y = 1$

methodical, enabling interested individuals to apply it immediately to solve their NLPDEs. The results of this study suggest that the proposed method is promising for exploring various soliton solutions of nonlinear equations in optical physics. Secondly, similar two-dimensional PDSs were developed, and the equilibrium points of the system were determined through the application of bifurcation theory. Examination was conducted on the periodic, quasi-periodic, and chaotic responses of traveling waves under the influence of an external periodic disturbance. As the intensity of the periodic disturbance increases, the perturbed system

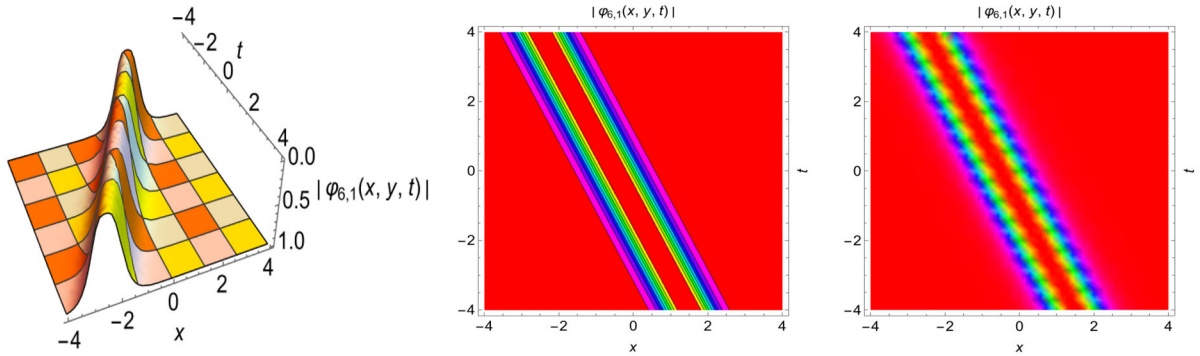


Fig. 16 The 3D, contour, and density plots for the solution $\left|\varphi_{6,1}(x, y, t)\right|$ in (73) when $b_1 = -2$, $b_2 = 1$, $b_3 = -2$, $\rho = 2$, $c = 2$, and $y = 1$

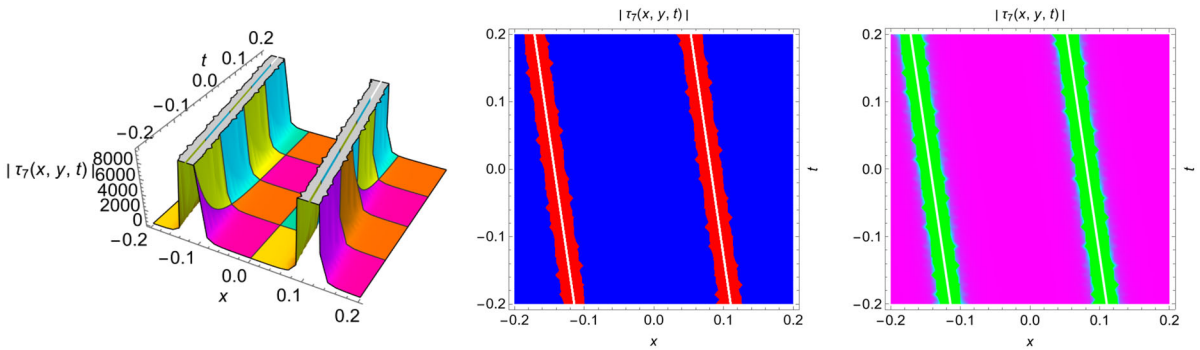


Fig. 17 The 3D, contour, and density plots for the solution $|\tau_7(x, y, t)|$ in (83) when $b_1 = 1$, $b_2 = 1$, $b_3 = 3$, $\rho = 2$, $c = 7$, and $y = 1$

exhibits a transition to quasi-periodic behavior, leading to chaos. The occurrence of quasi-periodic and chaotic movements was documented in the presence of an external perturbation term, with sensitivity analysis employed to validate the findings. Graphs were drawn using the Maple program.

The soliton solutions we obtain are new and unique for the (2+1)-dimensional cmKdV system. Also, compared to many other works, our findings contain a more comprehensive range of functions, including trigonometric, hyperbolic, exponential, etc. Moreover, these accepted solutions will apply to studying analytically NLPDEs in mathematical physics, plasma physics, applied sciences, non-linear dynamics, and engineering. In the future, we could explore the stability and long-term behavior of the identified solitary wave solutions in more detail. Additionally, examining how different parameters affect the system dynamics may help us discover more interesting phenomena. With Maple's assistance, we double-checked the results by substituting them back into the original formula.

Author contributions Bahadır Kopçasız: Software; visualization; writing—original draft; methodology; validation; conceptualization.

Funding Open access funding provided by the Scientific and Technological Research Council of Türkiye (TÜBİTAK). There is no funding for this work.

Data availability All data generated or analyzed during this study are included in this published article.

Declarations

Conflict of interest The author declares that there is no conflict of interest.

Open Access This article is licensed under a Creative Commons Attribution 4.0 International License, which permits use, sharing, adaptation, distribution and reproduction in any medium or format, as long as you give appropriate credit to the original

author(s) and the source, provide a link to the Creative Commons licence, and indicate if changes were made. The images or other third party material in this article are included in the article's Creative Commons licence, unless indicated otherwise in a credit line to the material. If material is not included in the article's Creative Commons licence and your intended use is not permitted by statutory regulation or exceeds the permitted use, you will need to obtain permission directly from the copyright holder. To view a copy of this licence, visit http://creativecommons.org/licenses/by/4.0/.

References

1. Li, L., Cheng, B., Dai, Z.: Novel evolutionary behaviors of N-soliton solutions for the (3+1)-dimensional generalized Camassa–Holm–Kadomtsev–Petciashvili equation. Nonlinear Dyn. **112**(3), 2157–2173 (2024)
2. Shao, H., Bilige, S.: Localized wave solutions and localized-kink solutions to a (3+1)-dimensional nonlinear evolution equation. Nonlinear Dyn. **112**, 3749 (2024)
3. Liu, H.D., Tian, B., Feng, S.P., Chen, Y.Q., Zhou, T.Y.: Integrability, bilinearization, Bäcklund transformations and solutions for a generalized variable-coefficient Gardner equation with an external-force term in a fluid or plasma. Nonlinear Dyn. **112**, 12345–12359 (2024)
4. Jawad, A.J.A.M., Biswas, A., Yildirim, Y., Alshomrani, A.S.: Optical solitons with differential group delay and intermodal dispersion singlet. Contemp. Math. **5**, 1054–1071 (2024)
5. Islam, M.T., Akter, M.A., Ryehan, S., Gómez-Aguilar, J.F., Akbar, M.A.: A variety of solitons on the oceans exposed by the Kadomtsev Petviashvili-modified equal width equation adopting different techniques. J. Ocean Eng. Sci. (2022)
6. Ali, A., Ahmad, J., Javed, S.: Exact soliton solutions and stability analysis to (3+1)-dimensional nonlinear Schrödinger model. Alex. Eng. J. **76**, 747–56 (2023)
7. Ali, A., Ahmad, J., Javed, S.: Exploring the dynamic nature of soliton solutions to the fractional coupled nonlinear Schrödinger model with their sensitivity analysis. Opt. Quantum Electron. **55**(9), 810 (2023)
8. Ali, A., Ahmad, J., Javed, S., Alkarni, S., Shah, N.A.: Investigate the dynamic nature of soliton solutions and bifurcation analysis to a new generalized two-dimensional nonlinear wave equation with its stability. Results Phys. **53**, 106922 (2023)
9. Javed, S., Ali, A., Ahmad, J., Hussain, R.: Study the dynamic behavior of bifurcation, chaos, time series analysis and soliton solutions to a Hirota model. Opt. Quantum Electron. **55**(12), 1114 (2023)
10. Bilal, M., Ren, J.: Dynamics of exact solitary wave solutions to the conformable time-space fractional model with reliable analytical approaches. Opt. Quantum Electron. **54**(1), 40 (2022)
11. Bilal, M., Ahmad, J.: Dispersive solitary wave solutions for the dynamical soliton model by three versatile analytical mathematical methods. Eur. Phys. J. Plus **137**(6), 674 (2022)
12. Bilal, M., Hu, W., Ren, J.: Different wave structures to the Chen–Lee–Liu equation of monomode fibers and its modulation instability analysis. Eur. Phys. J. Plus **136**, 1–15 (2021)
13. Bilal, M., Younas, U., Ren, J.: Dynamics of exact soliton solutions to the coupled nonlinear system using reliable analytical mathematical approaches. Commun. Theor. Phys. **73**(8), 085005 (2021)
14. Bilal, M., Ahmad, J.: A variety of exact optical soliton solutions to the generalized (2+1)-dimensional dynamical conformable fractional Schrödinger model. Res. Phys. **33**, 105198 (2022)
15. Islam, S.R.: Bifurcation analysis and soliton solutions to the doubly dispersive equation in elastic inhomogeneous Murnaghan's rod. Sci. Rep. **14**(1), 11428 (2024)
16. Rayhanul Islam, S.M., Khan, K.: Investigating wave solutions and impact of nonlinearity: comprehensive study of the KP-BBM model with bifurcation analysis. PLoS One **19**(5), e0300435 (2024)
17. Rayhanul Islam, S.M., Yiasir Arafat, S.M., Inc, M.: Exploring novel optical soliton solutions for the stochastic chiral nonlinear Schrö dinger equation: stability analysis and impact of parameters. J. Nonlinear Opt. Phys. Mater. 2450009 (2024)
18. Islam, S.R.: Bifurcation analysis and exact wave solutions of the nano-ionic currents equation: via two analytical techniques. Results Phys. **58**, 107536 (2024)
19. Islam, S.R., Khan, K., Akbar, M.A.: Optical soliton solutions, bifurcation, and stability analysis of the Chen–Lee–Liu model. Results Phys. **51**, 106620 (2023)
20. Adel, M., Tariq, K.U., Ahmad, H., Kazmi, S.R.: Soliton solutions, stability, and modulation instability of the (2+1)-dimensional nonlinear hyperbolic Schrödinger model. Opt. Quantum Electron. **56**(2), 182 (2024)
21. Wazwaz, A.M.: Multiple soliton solutions and other exact solutions for a two-mode KdV equation. Math. Methods Appl. Sci. **40**, 2277–2283 (2017)
22. Triki, H., Ak, T., Moshokoa, S., Biswas, A.: Soliton solutions to KdV equation with spatio-temporal dispersion. Ocean Eng. **114**, 192–203 (2016)
23. Yıldırım, Y., Yaşar, E.: An extended Korteweg–de Vries equation: multi-soliton solutions and conservation laws. Nonlinear Dyn. **90**, 1571–1579 (2017)
24. Refaie Ali, A., Alam, M.N., Parven, M.W.: Unveiling optical soliton solutions and bifurcation analysis in the space-time fractional Fokas–Lenells equation via SSE approach. Sci. Rep. **14**(1), 2000 (2024)
25. Akram, G., Sadaf, M., Arshed, S., Farrukh, M.: Optical soliton solutions of Manakov model arising in the description of wave propagation through optical fibers. Opt. Quantum Electron. **56**(5), 906 (2024)
26. Islam, M.T., Sarkar, T.R., Abdullah, F.A., Gómez-Aguilar, J.F.: Distinct optical soliton solutions to the fractional Hirota Maccari system through two separate strategies. Optik **300**, 171656 (2024)
27. Muhammad, U.A., Sabi'u, J., Salahshour, S., Rezazadeh, H.: Soliton solutions of (2+1) complex modified Korteweg–de Vries system using improved Sardar method. Opt. Quantum Electron. **56**(5), 802 (2024)
28. Myrzakulov, R., Mamyrbekova, G., Nugmanova, G., Lakshmanan, M.: Integrable (2+1)-dimensional spin models with self-consistent potentials. Symmetry **7**(3), 1352–1375 (2015)
29. Yesmakhanova, K., Shaikhova, G., Bekova, G., Myrzakulov, R.: Darboux transformation and soliton solution for the

(2+1)-dimensional complex modified Korteweg–de Vries equations. In: Journal of Physics: Conference Series, vol. 936, no. 1, p. 012045. IOP Publishing (2017)
30. Yuan, F., Zhu, X., Wang, Y.: Deformed solitons of a typical set of (2+1)-dimensional complex modified Korteweg–de Vries equations. Int. J. Appl. Math. Comput. Sci. **30**, 337 (2020)
31. Yuan, F.: The order-n breather and degenerate breather solutions of the (2+1)-dimensional cmKdV equations. Int. J. Mod. Phys. B **35**(04), 2150053 (2021)
32. Shaikhova, G., Serikbayev, N., Yesmakhanova, K., Myrzakulov, R.: Nonlocal complex modified Korteweg–de Vries equations: reductions and exact solutions. In: Proceedings of the Twenty-First International Conference on Geometry, Integrability and Quantization, vol. 21, pp. 265–272. Bulgarian Academy of Sciences, Institute for Nuclear Research and Nuclear Energy (2020)
33. Shaikhova, G., Kutum, B., Myrzakulov, R.: Periodic traveling wave, bright and dark soliton solutions of the (2+1)-dimensional complex modified Korteweg–de Vries system of equations by using three different methods. AIMS Math. **7**(10), 18948–18970 (2022)
34. Ghanbari, B., Baleanu, D.: Applications of two novel techniques in finding optical soliton solutions of modified nonlinear Schrödinger equations. Res. Phys. **44**, 106171 (2023)
35. Khan, A., Saifullah, S., Ahmad, S., Khan, M.A., Rahman, M.U.: Dynamical properties and new optical soliton solutions of a generalized nonlinear Schrödinger equation. Eur. Phys. J. Plus. **138**(11), 1059 (2023)
36. Ur Rahman, M., Sun, M., Boulaaras, S., Baleanu, D.: Bifurcations, chaotic behavior, sensitivity analysis, and various soliton solutions for the extended nonlinear Schrödinger equation. Bound. Value Probl. **2024**(1), 1–15 (2024)
37. Tang, L., Biswas, A., Yildirim, Y., Asiri, A.: Bifurcation analysis and chaotic behavior of the concatenation model with power-law nonlinearity. Contemp. Math. **4**(4), 1014–1025 (2023)
38. Ali, A., Hussain, R., Javed, S.: Exploring the dynamics of Lie symmetry, Bifurcation and Sensitivity analysis to the nonlinear Schrö dinger model. Chaos Solitons Fractals **180**, 114552 (2024)
39. Salam, M.A., Akbar, M.A., Ali, M.Z., Inc, M.: Dynamic behavior of positron acoustic multiple-solitons in an electron–positron-ion plasma. Opt. Quantum Electron. **56**(4), 623 (2024)
40. Jhangeer, A., Almusawa, H., Hussain, Z.: Bifurcation study and pattern formation analysis of a nonlinear dynamical system for chaotic behavior in traveling wave solution. Res. Phys. **37**, 105492 (2022)
41. Jhangeer, A., Muddassar, M., Rehman, Z.U., Awrejcewicz, J., Riaz, M.B.: Multistability and dynamic behavior of nonlinear wave solutions for analytical kink periodic and quasi-periodic wave structures in plasma physics. Res. Phys. **29**, 104735 (2021)
42. Natiq, H., Banerjee, S., Misra, A.P., Said, M.R.M.: Degenerating the butterfly attractor in a plasma perturbation model using nonlinear controllers. Chaos Solitons Fractals **122**, 58–68 (2019)
43. Muhammad, U.A., Sabi'u, J., Salahshour, S., Rezazadeh, H.: Soliton solutions of (2+1) complex modified Korteweg–de Vries system using improved Sardar method. Opt. Quantum Electron. **56**(5), 802 (2024)

Publisher's Note Springer Nature remains neutral with regard to jurisdictional claims in published maps and institutional affiliations.